GEOPHYSICS, VOL. 70, NO. 6 (NOVEMBER-DECEMBER 2005); P. 33ND–61ND, 6 FIGS.
10.1190/1.2133784

75th Anniversary

The historical development of the magnetic method in exploration

M. N. Nabighian[1], V. J. S. Grauch[2], R. O. Hansen[3], T. R. LaFehr[4], Y. Li[1], J. W. Peirce[5], J. D. Phillips[2], and M. E. Ruder[6]

ABSTRACT

The magnetic method, perhaps the oldest of geophysical exploration techniques, blossomed after the advent of airborne surveys in World War II. With improvements in instrumentation, navigation, and platform compensation, it is now possible to map the entire crustal section at a variety of scales, from strongly magnetic basement at regional scale to weakly magnetic sedimentary contacts at local scale. Methods of data filtering, display, and interpretation have also advanced, especially with the availability of low-cost, high-performance personal computers and color raster graphics. The magnetic method is the primary exploration tool in the search for minerals. In other arenas, the magnetic method has evolved from its sole use for mapping basement structure to include a wide range of new applications, such as locating intrasedimentary faults, defining subtle lithologic contacts, mapping salt domes in weakly magnetic sediments, and better defining targets through 3D inversion. These new applications have increased the method's utility in all realms of exploration — in the search for minerals, oil and gas, geothermal resources, and groundwater, and for a variety of other purposes such as natural hazards assessment, mapping impact structures, and engineering and environmental studies.

HISTORY OF MAGNETIC EXPLORATION

The earliest observations on magnets are supposedly traced back to the Greek philosopher Thales in the sixth century B.C.E. (Appendix A). The Chinese were using the magnetic compass around A.D. 1100, western Europeans by 1187, Arabs by 1220, and Scandinavians by 1300. Some speculate that the Chinese had discovered the orientating effect of magnetite, or lodestone as early as the fourth century B.C.E. and that Chinese ships had reached the east coast of India for the first time in 101 BCE using a navigational compass.

Sir William Gilbert (1540–1603) made the first investigation of terrestrial magnetism. In *De Magnete* (abbreviated title) he showed that the earth's magnetic field can be approximated by the field of a permanent magnet lying in a general north-south direction near the earth's rotational axis (Telford et al., 1990).

Manuscript received by the Editor May 19, 2005; revised manuscript received July 11, 2005; published online November 3, 2005.
[1]Colorado School of Mines, 1500 Illinois Street, Golden, Colorado 80401-1887. E-mail: mnabighi@mines.edu; ygli@mines.edu.
[2]U.S. Geological Survey, Box 25046, Federal Center MS 964, Denver, Colorado 80225. E-mail: tien@usgs.gov; jeff@usgs.gov.
[3]PRJ Inc., 12640 West Cedar Drive, Suite 100, Lakewood, Colorado 80228. E-mail: rohansen@prj.com.
[4]Colorado School of Mines (retired), 1500 Illinois Street, Golden, Colorado 80401-1887. E-mail: lafehr@bresnan.net.
[5]GEDCO, 1200, 815–8th Avenue SW, Calgary, Alberta, T2P 3E2, Canada. E-mail: jwpeirce@gedco.com.
[6]Wintermoon Geotechnologies, Inc., 280 Columbine Street, Suite 301, Denver, Colorado 80206. E-mail: meruder@wintermoon.com.

The attraction of compass needles to natural iron formations eventually led to their use as a prospecting tool by the 19th century. [1]

As the association between magnetite and base metal deposits became better understood, demand for more sensitive instruments grew. Until World War II, these instruments were mostly specialized adaptations of the vertical compass (dipping needle), although instruments based on rotating coil inductors were also developed and used both for ground and airborne surveys.

Victor Vacquier and his associates at Gulf Research and Development Company were key players in developing the first fluxgate magnetometer for use in airborne submarine detection during World War II (Reford and Sumner, 1964; Hanna, 1990). This instrument offered an order-of-magnitude improvement in sensitivity over previous designs. After the war, this improvement initiated a new era in the use of airborne magnetic surveys, both for the exploration industry and for government efforts to map regional geology at national scales (Hanna, 1990; Hood, 1990).

Oceanographers quickly adapted early airborne magnetometers to marine use. In 1948, Lamont Geological Observatory borrowed a gimbal-mounted fluxgate magnetometer from the U. S. Geological Survey and towed it across the Atlantic (Heezen et al., 1953). Scripps Institution of Oceanography began towing a similar instrument in late 1952 and in 1955 conducted the first 2D marine magnetic survey off the coast of southern California (Mason, 1958). This now-famous marine magnetic survey showed a pattern of magnetic stripes offset by a fracture zone: the stripes were later attributed to seafloor spreading during periods of geomagnetic reversals (Vine and Mathews, 1963; Morley and Larochelle, 1964).

As new instruments continued to be developed from the 1950s to 1970s, sensitivity was increased from around 1 nT for the proton precession magnetometer to 0.01 nT for alkali-vapor magnetometers. With higher sensitivities, the error budget for aeromagnetic surveys became dominated by location accuracy, heading errors, temporal variations of the magnetic field, and other external factors (e.g., Jensen, 1965). The development of magnetic gradiometer systems in the 1980s highlighted the problem of maneuver noise caused by both the ambient magnetic field of the platform and by currents induced in the platform while moving in the earth's magnetic field (Hardwick, 1984).

The availability of the Global Positioning System (GPS) by the early 1990s tremendously improved the location accuracy and thus the error budget of airborne surveys. At the same time, explorationists began to design airborne surveys so they could resolve subtle magnetic-field variations such as those caused by intrasedimentary sources (see papers in Peirce et al., 1998). The higher resolution was achieved primarily by tightening line spacing and lowering the flight altitude. Today, high-resolution aeromagnetic (HRAM) surveys are considered industry standard, although exactly what flight specifications constitute a high-resolution survey is ill defined. Typical exploration HRAM surveys have flight heights of 80–150 m and line spacings of 250–500 m (Millegan, 1998). Exploration surveys are generally flown lower in Australia, at 60–80 m above ground (e.g., Robson and Spencer, 1997), and even lower if acquired by the Geological Survey of Finland (30–40 m flight height with 200–m line spacing; http://www.gsf.fi/aerogeo/eng0.htm). (Airspace regulations, urban development, or rugged terrain prevent such low-altitude flying in many places.) In contrast to these typical exploration specifications, aeromagnetic studies that require high resolution of anomalies in plan view, such as those geared toward mapping complicated geology, usually entail uniform line spacings and flight heights, following the guidelines established by Reid (1980). Unmanned aerial systems are also becoming available and should be a cost-effective tool for acquiring low-altitude magnetic data in relatively unpopulated areas, although their eventual role in exploration is difficult to predict.

[1]There is a story that a Cretan shepherd named Magnes, while tending sheep on the slopes of Mount Ida, found that the nails of his boots were attracted to the ground. To find the source of the attraction he dug up the ground and found stones that we now refer to as lodestones.

THE EARTH'S MAGNETIC FIELD

The largest component (80–90%) of the earth's field is believed to originate from convection of liquid iron in the earth's outer core (Campbell, 1997), which is monitored and studied using a global network of magnetic observatories and various satellite magnetic surveys (Langel and Hinze, 1998). To a first approximation, this field is dipolar and has a strength of approximately 50 000 nT, but there are significant additional spherical harmonic components up to about order 13. Furthermore, this field changes slowly with time and is believed to undergo collapse, often followed by reversal, on a time scale of 100 000 years or so. Understanding the history of reversals, both as a pattern over time and in terms of decay and rebuilding of the primary dipole field, is the focus of paleomagnetic studies [see Cox (1973) and McElhinny (1973) for excellent historical perspectives].

Although the crustal field is the focus of exploration, magnetic fields external to the earth have a large effect on magnetic measurements and must be removed during data processing. These effects are the product of interaction between the global field and magnetic fields associated with solar wind (Campbell, 1997). First, the earth's field is compressed on the sunward side, giving rise to a daily (diurnal) variation; at midlatitudes, diurnal variations are roughly 60 nT. Second, the interaction generates electrically charged particles that maintain a persistent ring current along the equator, called the equatorial electrojet. Instabilities in the ring current give rise to unpredictable magnetic-field fluctuations of tens of nT near the earth's surface. Finally, near the poles, entrainment of charged particles along field lines creates strong magnetic-field fluctuations during magnetic storms on time scales of a few hours and with amplitudes in excess of 200 nT.

The remaining component of the earth's field originates in iron-bearing rocks near the earth's surface where temperatures are sufficiently low, i.e., less than about 580°C (the Curie temperature of magnetite). This region is confined to the upper 20–30 km of the crust. The crustal field, its relation to the distribution of magnetic minerals within the crust, and the information this relation provides about exploration targets are the primary subjects of the magnetic method in exploration.

APPLICATIONS OF MAGNETIC MEASUREMENTS

Magnetic measurements for exploration are acquired from the ground, in the air, on the ocean, in space, and down boreholes, covering a large range of scales and for a wide variety of purposes. Measurements acquired from all but the borehole platform focus on variations in the magnetic field produced by lateral variations in the magnetization of the crust. Borehole measurements focus on vertical variations in the vicinity of the borehole.

Ground and airborne magnetic surveys

Ground and airborne magnetic surveys are used at just about every conceivable scale and for a wide range of purposes. In exploration, they historically have been employed chiefly in the search for minerals. Regional and detailed magnetic surveys continue to be a primary mineral exploration tool in the search for diverse commodities, such as iron, base and precious metals, diamonds, molybdenum, and titanium. Historically, ground surveys and today primarily airborne surveys are used for the direct detection of mineralization such as iron oxide–copper–gold (FeO-Cu-Au) deposits, skarns, massive sulfides, and heavy mineral sands; for locating favorable host rocks or environments such as carbonatites, kimberlites, porphyritic intrusions, faulting, and hydrothermal alteration; and for general geologic mapping of prospective areas. Aeromagnetic surveys coupled with geologic insights were the primary tools in discovering the Far West Rand Goldfields gold system, one of the most productive systems in history (Roux, 1970). Kimberlites (the host rock for diamonds) are explored successfully using high-resolution aeromagnetic surveys (positive or negative anomalies, depending on magnetization contrasts) (Macnae, 1979; Keating, 1995; Power et al., 2004).

Another economically important use of the magnetic method is the mapping of buried igneous bodies. These generally have higher susceptibilities than the rocks that they intrude, so it is often easy to map them in plan view. Commonly, the approximate 3D geometry of the body can also be determined. Because igneous bodies are frequently associated with mineralization, a magnetic interpretation can be the first step in finding areas favorable for the existence of a mineral deposit. In sedimentary basins, buried igneous bodies may have destroyed hydrocarbon deposits in their immediate vicinity, their seismic signature can be mistaken for a sedimentary structure (Chapin et al., 1998), or their orientation is important in understanding structural traps in an area (e.g., the Eocene Lethbridge dikes in southern Alberta, Canada). Igneous bodies can also form structural traps for subsequent hydrocarbon generation. For example, brecciated igneous rocks [e.g., Eagle Springs Field, Nevada; Fabero Field, Mexico; Badejo and Linguado Fields, Brazil; Jatibarang Field, Indonesia; and reported potential in the Taranaki Basin, New Zealand, all cited in Batchelor and Gutmanis (2002)] are known to be reservoirs.

For regional exploration, magnetic measurements are important for understanding the tectonic setting. For example, continental terrane boundaries are commonly recognized by the contrast in magnetic fabric across the line of contact (e.g., Ross et al., 1994; examples in Finn, 2002). Such regional interpretations require continent-scale magnetic databases. Development of these databases commonly involves merging numerous individual aeromagnetic surveys with highly variable specifications and quality. Such efforts have been ongoing for decades. For example, two major compilations have been completed for North America (Committee for the Magnetic Anomaly Map of North America, 1987; North American Magnetic Anomaly Group, 2002), which updated earlier efforts for the United States (Zietz, 1982) and Canada (Teskey et al., 1993). A comprehensive, near-global compilation of magnetic data outside the United States, Canada, Australia, and the Arctic regions was undertaken in a series of projects by the University of Leeds, the International Institute for Geo-Information Science and Earth Observation (ITC), and commercial partners (Fairhead et al., 1997).

Several countries (e.g., Australia, Canada, Finland, Sweden, and Norway) have vigorous government programs to develop countrywide, modern, high-resolution aeromagnetic databases, which include data acquisition and merging of data from individual surveys. These efforts have been successful in promoting mineral exploration and facilitating ore deposit discoveries.

The study of basin structure is an important economic application of magnetic surveys, especially in oil and gas exploration. For the most part, basin fill typically has a much lower susceptibility than the crystalline basement. Thus, it is commonly possible to estimate the depth to basement and, under favorable circumstances, quantitatively map basement structures, such as faults and horst blocks (e.g., Prieto and Morton, 2003). Since structure in shallower sections often lies conformably over the basement, at least to some depth, and faulting in shallower sections is often controlled by reactivation of basement faults, it is often possible to identify structures favorable to hydrocarbon accumulation from basement interpretation.

With the advent of HRAM surveys and the subnanotesla resolution they offer, it is now possible to map intrasedimentary faults by identifying their small and complex magnetic anomalies that occur where there are "marker beds" containing greater than average quantities of magnetite. Displacement of these marker beds generates modest (a few tenths to about 10 nT at 150 m elevation) anomalies that can be used to trace corresponding fault systems. The complex nature of these anomalies is illustrated in a case history in the Albuquerque Basin (see Case Histories section) where the magnetizations are high enough to clearly understand the relationships of bed thickness, offset, fault dip, etc. (Grauch et al., 2001). In hydrocarbon exploration, such techniques can be used to help correlate complex fault systems for exploration (Spaid-Reitz and Eick, 1998; Peirce et al., 1999) or for reservoir development (see Case Histories section; Goussev et al., 2004). In areas where beds carrying a magnetic signature dip at a significant angle, a good magnetic survey can be used to map surface geology very precisely (e.g., Abaco and Lawton, 2003).

The magnetic method has thus expanded from its initial use solely as a tool for finding iron ore to a common tool used in exploration for minerals, hydrocarbons, ground water, and geothermal resources. The method is also widely used in additional applications such as studies focused on water-resource assessment (Smith and Pratt, 2003; Blakely et al., 2000a), environmental contamination issues (Smith et al., 2000), seismic hazards (Blakely et al., 2000b; Saltus et al., 2001; Langenheim et al., 2004), park stewardship (Finn and Morgan,

2002), geothermal resources (Smith et al., 2002), volcano-related landslide hazards (Finn et al., 2001), regional and local geologic mapping (Finn, 2002), mapping of unexploded ordnances (Butler, 2001), locating buried pipelines (McConnell et al., 1999), archaeological mapping (Tsokas and Papazachos, 1992), and delineating impact structures (Campos-Enriquez et al., 1996; Goussev et al., 2003), which can sometimes be of economic importance (Mazur et al., 2000).

Borehole magnetic surveys

Borehole measurements of magnetic susceptibility and of the three orthogonal components of the magnetic field began in the early 1950s (Broding et al., 1952). Both types of measurements can be used to determine rock magnetic properties, which aids in geologic correlation between wells. However, magnetic-field measurements in boreholes also can be used to determine both location and orientation of magnetic bodies missed by previous drilling. Levanto (1959) describes the use of three-component fluxgate magnetometers to determine the extension of magnetic ore bodies.

Interpretation of borehole magnetic surveys was originally accomplished graphically by plotting the field lines along the borehole, extrapolating them outside the borehole, and looking for areas of field-line convergence. Least-square techniques were also employed to determine the parameters of the magnetic body (Silva and Hohmann, 1981). Today, acquisition of borehole magnetic surveys is not common practice, perhaps owing to the expense required in accurately determining borehole azimuth and dip.

Marine magnetic surveys

Marine magnetic measurements began at Lamont in the late 1940s (Oreskes, 2001) and led to the development of the Vine-Matthews-Morley model of seafloor spreading (Dietz, 1961; Hess, 1962; Vine and Matthews, 1963; and Morley and Larochelle, 1964). The name of this model has been updated by consensus (Vine, 2001) to recognize Larry Morley of the Geological Survey of Canada as the independent developer of the theory of seafloor spreading (Morley's original paper, which was rejected in early 1963, is reproduced in Morley, 2001). In fact, these marine magnetic measurements were a major factor in the acceptance of both the plate-tectonic theory and of the dynamo theory of generation of the earth's core field.

The seafloor spreading model is based on the concept that the seafloor is magnetized either positively or negatively, depending on the polarity epoch of the earth's magnetic field. New seafloor is created at mid-ocean ridges and becomes part of oceanic plates moving away from the spreading center. Thus, magnetic anomalies along a section transverse to the spreading center show a regular pattern of highs and lows (stripes) — often symmetric about the spreading center — that can be calibrated in age to the geomagnetic timescale (this timescale was new and unproven in 1963; a more recent compilation accompanies the Geological Society of America's 1999 geologic timescale). Leg 3 of the original Deep Sea Drilling Project (Maxwell and von Herzen et al., 1970) was designed to test the theory of sea-floor spreading by comparing the paleontological ages of the oldest sediments in the South Atlantic Ocean to the ages predicted by the seafloor spreading hypothesis. The two sets of ages matched very well, and the Vine-Matthews-Morley model was generally accepted; plate tectonics became a new paradigm in earth sciences.

Marine magnetic measurements also are routinely used for normal exploration applications, although not in the volume of aeromagnetic work.

Satellite magnetic measurements

Magnetic surveying entered the space age in 1964 with the launch of a scalar magnetometer on the Cosmos 49 mission. Subsequently, the POGO suite of polar-orbiting satellites, OGO-2, OGO-4, and OGO-6, conducted scalar measurements over a seven-year period. Magsat, flown in 1979–1980 in polar orbit, carried the first vector magnetometer. Satellite DE-1 collected vector information as well, in spite of its highly elliptical orbit (500 km to 22,000 km perigee and apogee, respectively). Recent launches in 1999 and 2000 of the Oersted (Olsen et al., 2000), CHAMP (Reigber et al., 2002), and Oersted-2/SAC-C missions were equipped with more sensitive scalar and vector magnetometers and have furthered our understanding of the core, crustal, and external fields.

Since 1970, satellite measurements of the geomagnetic field have been used to better model the dynamics of the core field and its secular variation. These models have been incorporated into the International Geomagnetic Reference Field (IGRF) (see Magnetic Data Processing section) to provide more accurate information for processing exploration-quality magnetic surveys. Satellite magnetometers have provided new insights into the external magnetic field as well. Although explorationists are not using satellite magnetic measurements for prospect generation and for mapping of the crustal field, we are reaping great benefits from their impact on the core field model and its regular five-year updates. In recent years, the magnetic method has formed an important component of extraterrestrial exploration (see the special section in the August 2003 issue of THE LEADING EDGE).

From planetary scales to areas of a few meters, the magnetic method has had a role to play, in some cases a decisive one. It could be argued that no other geophysical method has such a broad range of applicability or offers such economical information.

MAGNETIC INSTRUMENTATION

Historical instruments

The Swedish mining compass was one of the earliest magnetic prospecting instruments. Developed in the mid-nineteenth century, it consisted of a light needle suspended in such a way as to allow it to move in both horizontal and vertical directions. An improved version, the American mining compass, was developed around 1860. These were the first in a class of so-called dipping-needle instruments with automatic meridian adjustment.

Although still in use these instruments were soon replaced by earth inductors, which could measure both the inclination and the various components of the earth's magnetic field from the voltage induced in a rotating coil. In 1936, Logachev (1946) used such a device with a sensitivity of about 1000 nT over the Kursk iron-ore deposit (Reford and Sumner, 1964). Soon after, the Schmidt vertical magnetometer was developed, which could measure the vertical component of the

earth's magnetic field using a magnetic system (rhomb-shaped needle) oriented at a right angle to the magnetic meridian; it measured the system dip through a mirror attached to the needle and an autocollimation telescope system. The vertical magnetometer was followed by the Schmidt horizontal magnetometer, which measured the horizontal component of the earth's field. Both instruments had an accuracy of 10–20 nT. The Schmidt magnetometers came to be known as Askania-Schmidt magnetometers.

In 1910, Edelman designed a vertical balance to be used in a balloon (Heiland, 1935). In 1946, a vertical-intensity magnetometer of the earth-inductor type was introduced by Lundberg (1947) for helicopter surveys, and a vibrating coil variety of the earth-inductor magnetometer was developed for both airborne and shipborne use (Frowe, 1948).

A complete description of early magnetic prospecting instruments and their uses can be found in Heiland (1940), Jakosky (1950), and Reford and Sumner (1964).

Fluxgate magnetometer

The fluxgate magnetometer was developed during World War II for airborne antisubmarine warfare applications; after the war, it was immediately adopted for exploration geophysics and remained the primary airborne instrument until the proton precession magnetometer was introduced in the 1960s.

Fluxgate magnetometers today have two major applications. In airborne systems they are used in a strap-down (nonoriented) configuration to perform heading corrections by measuring the altitude of the aircraft in the earth's field. They are also the dominant instrument in downhole applications because of their small size, ruggedness, and ability to tolerate high temperatures.

The basic elements of a fluxgate magnetometer are two matched cores of highly permeable material, typically ferrite, with primary and secondary windings around each core. The primary windings are connected in series but with opposite orientations and are driven by a 50–1000-Hz current which saturates the cores in opposite directions, twice per cycle. The secondary coils are connected to a differential amplifier to measure the difference between the magnetic field produced in the two cores. This signal is asymmetrical because of the ambient magnetic field along the core axis, producing a spike at twice the input frequency whose amplitude is proportional (for small imbalances) to the field along the core axis. A detailed discussion of the fluxgate magnetometer can be found in Telford et al. (1990).

Typically, fluxgate elements are packaged into sets of three core pairs with orthogonal axes, so all three components of the earth's field can be measured. The resolution of a fluxgate system is dependent on the accuracy with which the cores and windings can be matched, hysteresis in the cores, and related effects; nevertheless, fluxgate units with better than 1 nT sensitivity are widely available. They are rugged, lightweight, and can be operated at relatively high measurement rates. Their major disadvantage for airborne applications is that because they are component instruments, they must be oriented. At least until recently, the accuracy of fluxgate measurements was limited by the stability of the gyro tables on which they were mounted.

Proton precession magnetometer

Proton precession magnetometers were introduced in the mid-1950s, and by the mid-1960s had supplanted fluxgate magnetometers for almost all exploration applications. Proton precession magnetometers do not require orientation, a great advantage over earlier devices.

The proton precession magnetometer is based on the splitting of nuclear spin states into substates in the presence of an ambient magnetic field by an amount proportional to the intensity of the field and a proportionality factor (the nuclear gyromagnetic ratio), which depends only on fundamental physical constants. The sensor consists of a quantity of material with odd nuclear spin, almost always hydrogen. The actual sensor filling is usually charcoal lighter fluid, decane, benzene, or, if necessary, even water.

The sensor is surrounded by a coil through which a dc current is applied. This induces transitions to the higher energy of two nuclear spin substates. The current is then turned off and used to detect the fields associated with the transition back to the lower of the spin substates. This transition emits an electromagnetic field whose frequency is proportional to the earth's field intensity, around 2 kHz. A frequency counter is then used to measure the field strength. The full treatment of the physics behind proton precession magnetometers (Hall, 1962) is usually explained intuitively in textbooks by envisioning the transition between nuclear substates as a precession of the nuclear magnetic moments around the earth's field direction at an angular frequency proportional to the intensity of the field.

The proton precession magnetometer has a number of advantages: it is rugged, simple, has essentially no intrinsic heading error, and does not require an orienting platform. However, to obtain reasonable signal strength, a fairly large quantity of sensor liquid and a large coil are required, making the instrument somewhat heavy, bulky, and power hungry. Furthermore, because a significant polarizing time is required and because the output signal is only around 2 kHz, the sample rate is somewhat limited if reasonable sensitivity is required. The best airborne units (now out of production) had a sensitivity of 0.05 nT at 2 Hz. More typical values would be 0.1 nT at 0.2 Hz for portable instruments still in use.

A variant (the Overhauser magnetometer) uses radio-frequency excitation and effectively displays continuous oscillation, which can be sampled at 5 Hz with resolution of 0.01 nT. The Overhauser variant also offers the lowest power drain of any modern magnetometer, a small sensor head, and minimal heading error. It is widely used in subsea magnetometers and is also used for airborne and ground survey work, often in gradient arrays.

Alkali vapor magnetometer

Alkali vapor magnetometers, with sensitivities around 0.01 nT and sample rates of 10 Hz, appeared in laboratories about the same time that proton precession magnetometers became popular field instruments. Because they were more fragile than proton precession magnetometers, and because the increased sensitivity was of marginal value, their use as field instruments was mostly restricted to gradiometers until the late 1970s. Today, alkali vapor magnetometers are the dominant instrument used for magnetic

surveys, although some proton precession instruments are still in use for ground surveys, and fluxgates are used for borehole surveys. The operating principle and the actual construction of alkali vapor magnetometers are somewhat complex. However, since they have become the dominant type in current airborne, shipborne, and ground exploration, a summary explanation of their operation is appropriate.

The sensing medium is an alkali vapor consisting of atoms randomly distributed between two different atomic-energy levels, separated by energy equivalent to a visible frequency. In the presence of a magnetic field, the most stable energy level is split (Zeeman splitting) by an amount proportional to the magnitude of the field. For ambient fields of around 50 000 nT, the splitting energy will correspond to a frequency in the range of a few hundred kHz, i.e., the AM radio band.

By shining light of the correct frequency through a vapor of a single-valence atom such as cesium or potassium, all of the electrons are forced into the higher-energy component of the split state (optical pumping). When this absorption is complete, the glass cell in which the vapor is contained becomes transparent because there are no further electrons to absorb the pumping radiation.

Now, a radio-frequency field is applied to this cell. If the field is of exactly the right frequency, the electrons are redistributed back to the lower level, and the cell becomes opaque. The correct frequency depends on the ambient magnetic-field strength, so a swept-frequency field is applied, and the precise frequency at which opacity occurs is used to derive the ambient-field intensity.

Alkali vapor instruments have excellent sensitivity, better than 0.01 nT. Because the frequency can be swept rapidly, 10-Hz sample rates are typical, and considerably higher ones are possible. These features account for the overwhelming popularity of this design. In addition, alkali vapor magnetometers are built to be lightweight and compact. The less desirable features are the fragility of the glass envelope and an intrinsic heading error. A good discussion of alkali vapor magnetometers can be found in Telford et al. (1990).

Superconducting quantum interference device (SQUID) magnetometer

The fact that a persistent current can exist in a superconducting loop has been known since the 1930s. This current is inherently insensitive to the ambient magnetic field; one of the main features of superconductors is that they expel external fields. Josephson (1962) showed that persistent currents could be maintained across small gaps in the superconducting loop and that the currents across the gap are sensitive to the magnetic flux passing through the loop. Flux is the product of the component of the magnetic field perpendicular to the loop and the loop area. Current changes can be monitored by a normal resonant circuit and used to obtain component field values. Instruments of this type are called superconducting quantum interference devices (SQUIDs) (Weinstock and Overton, 1981).

SQUIDs have not been widely used in magnetic field applications, although they have been used extensively in magnetotelluric and paleomagnetic studies and, recently, in both ground and airborne EM surveys as magnetic component sensors. The main reason is the need for cryogenic supplies, which reduces the mobility of SQUID magnetometers. Since the appearance of high-temperature superconductors, it has been anticipated that liquid nitrogen could be used as the cooling fluid, which is much easier to manufacture and handle than liquid helium. However, high-temperature SQUIDs have only recently appeared on the market. They have somewhat lower sensitivities than the liquid-helium instruments, primarily because the $1/f$ noise in the amplifier electronics is higher, but this should not be a major concern for most applications. It seems likely that the use of SQUIDs may increase in the near future, as shown by recent surveys flown in gradient mode for mineral surveys.

Stuart (1972) gives a comprehensive review of magnetic instruments used in geophysical applications. Grivet and Malnar (1967) give detailed discussions of instruments based on Zeeman splitting, including proton precession magnetometers, alkali vapor magnetometers, and related designs, not limited to geophysical instruments.

ROCK-MAGNETIC PROPERTIES

In geologic interpretation of magnetic data, knowledge of rock-magnetic properties for a particular study area requires an understanding of both magnetic susceptibility and remanent magnetization. Seventy-five years ago, studies were already underway to explain the geologic factors influencing rock-magnetic properties that produce magnetic anomalies (Slichter, 1929; Stearn, 1929a). Factors influencing rock-magnetic properties for various rock types are summarized by Haggerty (1979), McIntyre (1980), Clark (1983, 1997), Bath and Jahren (1984), Grant (1985), Reynolds et al. (1990a), and Clark and Emerson (1991). The Norwegian, Swedish, and Finnish surveys have been amassing large amounts of rock-property information in conjunction with their national geophysical programs. Several studies have focused on developing classification schemes based on the statistical correlations between rock types and these petrophysical measurements (Korhonen et al., 2003).

Less progress has been made in understanding how information on magnetic properties measured from hand samples can be transferred to scales more appropriate for aeromagnetic interpretation. Reford and Sumner (1964) and Clark (1983) discussed how the high variability of properties measured in hand samples contradicts the apparent homogeneity in the bulk effects of large bodies at the scale of aeromagnetic studies. Understanding this contradiction remains elusive, especially in understanding sedimentary sources. Improved understanding may result from case studies that directly investigate the relationship between magnetic anomalies, rock properties, and geology (Abaco and Lawton, 2003; Davies et al., 2004).

The importance of sedimentary sources of magnetic anomalies was the subject of considerable discussion before the end of World War II (e.g., Jenny, 1936; Wantland, 1944). Magnetic anomalies produced by glacial till were also widely known (summarized in Gay, 2004). However, experience with the relatively low resolution of the early aeromagnetic data allowed workers to effectively ignore their effects (Steenland, 1965; Nettleton, 1971), giving rise to the misconception that sediments are nonmagnetic. As data resolution increased, magnetic anomalies arising from sedimentary sources were again recognized (Grant, 1972). This recognition gained prominence in the 1980s, when studies were initiated to test

for magnetic effects related to hydrocarbon seepage. These and subsequent studies demonstrated that magnetization capable of producing aeromagnetic anomalies in clastic sedimentary rocks and sediments arise from the abundance of detrital magnetite (Reynolds, Rosenbaum et al., 1990, 1991; Gay and Hawley, 1991; Gunn, 1997, 1998; Wilson et al., 1997; Grauch et al., 2001; Abaco and Lawton, 2003), remanence residing in iron sulfides that replaced the original detrital material (Reynolds, Rosenbaum et al., 1990, 1991), or possibly some other kind of remanence (Phillips et al., 1998). A recent study of the Edwards aquifer in central Texas has revealed, in a low-level helicopter survey, that carbonates may also contain enough detrital magnetite to produce magnetic anomalies at faults (Smith and Pratt, 2003).

At local scales, magnetite can be produced by microbial activity (Machel and Burton, 1991) or destroyed by sulfidization (Goldhaber and Reynolds, 1991) in processes related to hydrocarbon migration, although it is still debated whether this effect can be detected from airborne surveys (Gay, 1992; Reynolds et al., 1990; Millegan, 1998; Stone et al., 2004). Morgan (1998) postulates that weak aeromagnetic lows in oil fields of the Irish Sea are caused by complex migration and mixing of fluids with hydrocarbons that reduced the magnetization of the host sandstones.

The importance of remanent magnetization in magnetic interpretation has been recognized by many previous workers (see references in Zietz and Andreasen, 1967). To simplify analytical methods, remanent magnetization has been commonly neglected or assumed to be collinear with the induced component. Bath (1968) considered remanent and induced components within 25° of each other to be collinear for practical purposes. Although valid in many geologic situations, a common misconception is that only mafic igneous rocks have high remanence. Several rock-magnetic and aeromagnetic studies have shown that remanence can be very high in felsic ash-flow tuffs (Bath, 1968; Rosenbaum and Snyder, 1985; Reynolds, Rosenbaum et al., 1990a; Grauch et al., 1999; Finn and Morgan, 2002).

MAGNETIC DATA PROCESSING

Data processing includes everything done to the data between acquisition and the creation of an interpretable profile, map, or digital data set. Standard steps in the reduction of aeromagnetic data, some of which also apply to marine and ground data, include removal of heading error and lag, compensation for errors caused by the magnetic field of the platform, the removal of the effects of time-varying external fields, removal of the International Geomagnetic Reference Field, leveling using tie-lines, microleveling, and gridding. One comprehensive reference that summarizes most aspects of magnetic data processing is Blakely (1995).

Compensation

All moving-platform magnetic measurements are subject to errors caused by the magnetic field of the platform, whether from in situ magnetic properties of the platform or from currents induced in the platform while moving in the earth's magnetic field. In shipborne and helicopter surveys, these effects are typically minimized by mounting the sensor on a long tow cable, thereby reducing the errors caused by the magnetic field of the vehicle. Fixed-wing airborne operations, on the other hand, usually use rigid magnetometer installations, such as a stinger protruding from the rear of the aircraft. Fixed installations offer better control of the sensor location and have been the preferred configuration since the early days of airborne data acquisition.

The field of the aircraft is significant unless the aircraft has been extensively rebuilt. This problem is overcome by compensating for the platform field. Error models were developed during World War II but not published until much later (Leliak, 1961). Early compensation methods consisted of attaching bar magnets and strips of Permalloy near the sensor to approximately cancel the aircraft field (EG&G Geometrics, 1970s).

Later, feedback compensators were developed for military use (CAE, 1968, Study guide for the 9-term compensator: Tech. Doc. TD-2501, as cited in Hardwick, 1984). However, Hardwick (1984) pointed out in a landmark paper that these were unsuitable for geophysical use because they were limited to the frequency band appropriate for submarine detection.

Hardwick (1984) also noted that good compensation was crucial to the usefulness of the magnetic gradiometer systems then being built. He described a software compensation system that was eventually commercialized and is now in widespread use, even in single-sensor systems. Alternatives, such as postprocessing compensation, are also available. It is fair to say that, along with the introduction of GPS, the use of these more sophisticated compensation models has produced the largest improvement in data quality over the past 20 years.

Global field models

The main component of the measured magnetic field originates from the magnetic dynamo in the earth's outer core (Campbell, 1997). This field is primarily dipolar, with amplitude of around 50 000 nT, but spherical harmonic terms up to about order 13 are significant. Since the core field is almost always much larger than that of the crustal geology, and since it has a significant gradient in many parts of the world, it is desirable to remove a model of the global field from the data before further processing; this can be done as soon as all positioning errors are corrected.

The model most widely used today is the International Geomagnetic Reference Field (IGRF, Maus and Macmillan, 2005). It was established in 1968 and became widely used with the availability of digital data in the mid-1970s (Reford, 1980). In 1981 the IGRF was modified in order to be continuous for all dates after 1944 (Peddie, 1982, 1983; Paterson and Reeves, 1985; Langel, 1992). Today, the IGRF is updated every five years and includes coefficients for predicting the core field into the near future. Coefficients are available for the time period 1900 through 2005 (Barton, 1997; Macmillan et al., 2003). In practice today, the IGRF is calculated for every data point before any further processing. Prior to GPS navigation, however, it was common practice to level surveys first, then remove a trend based on the best fit, either to the data or to a few IGRF values. For many of the earliest analog surveys, an arbitrary (sometimes unspecified) constant was subtracted from the measured data solely as a matter of convenience before contouring.

In the future, the IGRF is likely to be supplanted by the Comprehensive Model (CM), which does a much better job of modeling time-varying fields from a variety of sources (Sabaka et al., 2002, 2004; Ravat et al., 2003).

External (time-varying) field removal

Ground-based and airborne surveys generally include a stationary magnetometer that simultaneously measures the stationary, time-varying magnetic field for later subtraction from the survey data (Hoylman, 1961; Whitham and Niblett, 1961; Morley, 1963; Reford and Sumner, 1964; Paterson and Reeves, 1985). There is still considerable debate on how many base stations are needed to adequately sample the spatial variations of the external field for larger surveys or when the survey area is at a considerable distance from the base of operations. At sea, it is generally not possible to have a base-station magnetometer in the survey area, and the problem is either ignored or measurements are made in a gradient mode. The measurement of multisensor gradiometer data can reduce the need for a base station because the common external signal at the two sensors is removed by the differencing process, but recovery of the total field data from the gradiometer data can be difficult (Breiner, 1981; Hansen, 1984; Paterson and Reeves, 1985). A method to fit distant base signals to the field signal in order to remove time-varying effects was proposed by O'Connel (2001) using a variable time-shift cross-correlator.

The leveling of surveys using tie-lines was originally developed as an alternative to the use of base-station data (Whitham and Niblett, 1961; Reford and Sumner, 1964; Mittal, 1984; Paterson and Reeves, 1985) but is now a standard step after base-station correction. The purpose of leveling today is to minimize residual differences in level between adjacent lines and long-wavelength errors along lines that inevitably remain after compensation and correction for external field variations by base station subtraction. These residual long-wavelength effects, even if small, can be visually distracting, particularly on image displays.

A set of tie-lines perpendicular to the main survey lines is normally acquired for leveling. The tie-line spacing is generally considerably greater than that of the main survey lines, although 1:1 ratios have been used where geologic features lack a dominant strike. The differences in field values at the intersections of the survey and tie-lines are calculated and corrections are applied to minimize these differences. A number of different strategies for computing these corrections are in use. Perhaps the most common is to calculate a constant correction for all lines by least-squares methods, sometimes augmented to a low-order polynomial. Other algorithms regard the tie-lines as fixed and adjust only the survey lines. All of these strategies are empirical, and no one method performs best under all circumstances.

Microleveling

Leveling, as described in the previous subsection, generally produces acceptable results for contour map displays, but small corrugations generally can still be seen on images. To suppress these, microleveling or decorrugation is applied (Hogg, 1979; Paterson and Reeves, 1985; Urquhart, 1988; Minty, 1991). One of the ironies of modern GPS navigation is that we know exactly where our data are located horizontally at the time of measurement, but we can only guess at the final observation surface after leveling and microleveling have been applied.

As in tie-line leveling, a number of microleveling algorithms are in use that differ in detail but all rely on the principle of removing the corrugation effects from a grid and using the decorrugated grid to correct the long-wavelength errors on the profile data. Because microleveling uses the grid in an essential way, it effectively erases the small corrugations. However, it also largely obliterates any features that actually trend along the survey lines.

Deculturing

Cultural anomalies are a serious problem in the geologic interpretation of airborne magnetic data, especially modern HRAM surveys that typically fly low above cultural sources. Many man-made structures (e.g., wells, pipelines, railroads, bridges, steel towers, and commercial buildings) are ferrous and so create sharp anomalies of tens to hundreds of nanoteslas. Cultural anomalies are often much larger in magnitude than the geologic anomalies of interest. Moreover, their shapes are effectively spikes with broadband frequency responses, making them difficult if not impossible to remove with linear filters.

Several approaches have been developed for cultural editing. The utility of each approach depends on the magnitude and type of cultural anomalies present. One approach is to avoid flying low-level surveys to suppress the cultural signal (Balsley, 1952), but this may diminish useful geological signals from shallow sources and does not eliminate noise spikes. The Naudy filter (Naudy and Dreyer, 1968) uses nonlinear filters to solve the problem. Hassan et al. (1998) discuss the relative merits and limitations of manual editing on a profile-by-profile basis, of semiautomatic filtering using a Naudy-type filter, and of fully automatic filtering using neural nets. Hassan and Peirce (2005) present an improved approach to manual editing for situations where good digital databases of existing culture are available. Wavelet filtering is another method that offers promise in terms of developing more effective automated techniques, but there will always be a need to manually oversee the results to prevent the removal of an important shallow geological signal.

For special cases where the source structure can be modeled, such as for well casings (Frischknecht et al., 1983; Boardman, 1985), it is possible to design effective automatic removal techniques (Dickinson, 1986; Pearson, 1996). However, all of these methods depend on recognition of a known anomaly signature. In general, it is not possible to construct such models; for example, the anomaly of a town is an aggregate of anomalies from many man-made sources, clearly beyond reasonable modeling capabilities. In such cases, it is necessary to resort to deleting the cultural anomaly from the data using flight-path video or digital cultural data as a guide and replacing it with interpolated values (Hassan and Peirce, 2005).

Gridding

Gridding of flight-line data is another area of continuing research. Because the density of data is so much greater along

the flight-line direction than across flight lines, early efforts concentrated on bidirectional interpolation (Bhattacharyya, 1969). Minimum curvature (Briggs, 1974) has proved to be a popular gridding algorithm for unaliased data. Present surveys are planned to minimize the amount of cross-track aliasing, following the guidelines of Reid (1980). However, for reconnaissance surveys and for fixed-wing surveys in areas of rough terrain, there will always be residual cross-track aliasing. An extension of the minimum-curvature-gridding algorithm designed to address this problem has recently been developed by O'Connell et al. (2005).

Another way to address the issue of flight-line data density is to use kriging with an anisotropic covariance function (Hansen, 1993). More exotic approaches use equivalent sources to produce a grid with the characteristics of a potential field (Cordell, 1992; Mendonça and Silva, 1994, 1995); others employ fractals (Keating, 1993) and wavelets (Ridsdill-Smith, 2000).

The evolution of magnetic data processing can be characterized more by the things we no longer need to discuss than those mentioned above. Included in the dustbin of earlier concerns are contouring algorithms, display hardware, camera- and map-based navigation, radio navigation systems, and base stations versus control lines.

ACCOUNTING FOR MAGNETIC TERRAIN

Rugged terrain poses a number of difficulties for data acquisition, processing, analysis, and interpretation (Hinze, 1985a). Data processing and acquisition errors caused by difficulties in flying over rugged terrain have been largely overcome with the advent of preplanned draped surfaces and GPS navigation, but these steps do not account for the effects of magnetic sources in the terrain itself. Magnetic anomalies produced by the magnetic effects of rocks that form topography are called topographic anomalies or magnetic terrain effects (Allingham, 1964; Grauch, 1987) and should not be confused with the effects produced by irregular terrain clearance. They are easily recognized by the strong correlation of the anomaly shapes to topography (Blakely and Grauch, 1983).

Magnetic terrain effects can severely mask the signatures of underlying sources, as demonstrated by Grauch and Cordell (1987). Many workers have attempted to remove or minimize magnetic terrain effects by using some form of filtering or modeling scheme (summarized in Grauch, 1987). Unlike gravity terrain corrections, however, these attempts have been successful only in favorable conditions. In more recent studies, workers have used rugged terrain to their advantage. In a basaltic volcanic field within the Rio Grande rift, for example, high-amplitude negative and positive anomalies correlate with topography and helped geologists distinguish similar-looking basalts with different ages (Thompson et al., 2002). At Mt. Rainier, the lack of magnetic anomalies correlating with terrain helped estimate the volume of hydrothermally altered material available for potential landslides (Finn et al., 2001).

MAGNETIC DATA FILTERING

The beginning stages of magnetic data interpretation generally involve the application of mathematical filters to observed data. The specific goals of these filters vary, depending on the situation. The general purpose is to enhance anomalies of interest and/or to gain some preliminary information on source location or magnetization. Most of these methods have a long history, preceding the computer age. Modern computing power has increased their efficiency and applicability tremendously, especially in the face of the ever-increasing quantity of digital data associated with modern airborne surveys.

Most filter and interpretation techniques are applicable to both gravity and magnetic data. As such, it is common, when applicable, to reference a paper describing a technique for filtering magnetic data when processing gravity data and vice versa.

Regional-residual separation

Regional-residual separation is a crucial step in the interpretation of magnetic data for mining or unexplored ordnance (UXO) applications but less so for petroleum applications because the depth range of hydrocarbon exploration extends throughout the sedimentary section. Historically, this problem was approached either by using a simple graphical approach (manually selecting data points to represent a smooth regional field) or by using various mathematical tools to obtain the regional field. This problem has been extensively treated for gravity data (Nabighian et al., 2005), and the proposed techniques apply equally well to magnetic investigations.

The graphical approach was initially limited to analyzing profile data and, to a lesser extent, gridded data. The earliest nongraphical approach considered the regional field at a point to be the average of observed values around a circle centered on the point; the residual field was simply the difference between this average value and the value observed at the central point (Griffin, 1949). Henderson and Zietz (1949) and Roy (1958) showed that this method was equivalent to calculating the second vertical derivative except for a constant factor. Agocs (1951) proposed using a least-squares polynomial fit to data to determine the regional field, an approach criticized by Skeels (1967) since the anomalies themselves will affect somewhat the determined regional. Zurflueh (1967) proposed using two-dimensional linear wavelength filters of different cutoff wavelengths. This method was further expanded by Agarwal and Kanasewich (1971), who also used a crosscorrelation function to obtain trend directions from magnetic data. A comprehensive discussion of application of Fourier transforms to potential field data can be found in Gunn (1975).

Syberg (1972a) described a matched-filter method for separating the residual field from the regional field. A method based on frequency-domain Wiener filtering for gravity data was proposed by Pawlowski and Hansen (1990) that is equally applicable to magnetic data. Matched filters and Wiener filters have much in common with other linear band-pass filters but have the distinct advantage of being optimal for a class of geologic models. Based on experience, however, it seems that significantly better results can be obtained using appropriate statistical geologic models than by attempting to adjust band the parameters of band-pass filter manually.

Li and Oldenburg (1998a) use a 3D magnetic inversion algorithm to invert the data over a large area in order to construct a regional susceptibility distribution from which a

regional field can then be calculated. In certain aspects, this method is a magnetic application of a gravity interpretation technique known as stripping (Hammer, 1963). Spector and Grant (1970) analyzed the shape of power spectra calculated from observed data. Clear breaks between low- and high-frequency components of the spectrum were used to design either band-pass or matched filters. In hydrocarbon exploration, this is the most common approach to separating different depth ranges of interest based on their frequency content. This approach is discussed in a modern context by Guspi and Introcaso (2000).

The existence of so many techniques for regional-residual separation proves that there are still some unresolved problems in this area. There is no single right answer for how to highlight one's target of interest.

Reduction to pole (RTP)

Like a gravity anomaly, the shape of a magnetic anomaly depends on the shape of the causative body. But unlike a gravity anomaly, a magnetic anomaly also depends on the inclination and declination of the body's magnetization, the inclination and declination of the local earth's magnetic field, and the orientation of the body with respect to magnetic north. To simplify anomaly shape, Baranov (1957) and Baranov and Naudy (1964) proposed a mathematical approach known as reduction to the pole. This method transforms the observed magnetic anomaly into the anomaly that would have been measured if the magnetization and ambient field were both vertical — as if the measurements were made at the magnetic pole. This method requires knowledge of the direction of magnetization, often assumed to be parallel to the ambient field, as would be the case if remanent magnetization is either negligible or aligned parallel to the ambient field. If such is not the case, the reduced-to-the-pole operation will yield unsatisfactory results. Reduction to the pole is now routinely applied to all data except for data collected at high magnetic latitudes.

The RTP operator becomes unstable at lower magnetic latitudes because of a singularity that appears when the azimuth of the body and the magnetic inclination both approach zero. Numerous approaches have been proposed to overcome this problem. Leu (1982) suggested reducing anomalies measured at low magnetic latitudes to the equator rather than the pole; this approach overcomes the instability, but anomaly shapes are difficult to interpret. Pearson and Skinner (1982) proposed a whitening approach that strongly reduced the peak amplitude of the RTP filter, thus reducing noise. Silva (1986) used equivalent sources, which gave good results but could become unwieldy for large-scale problems. Hansen and Pawlowski (1989) designed an approximately regulated filter using Wiener techniques that accounted well for noise. Mendonça and Silva (1993) used a truncated series approximation of the RTP operator. Gunn (1972, 1995) designed Wiener filters in the space domain by determining filter coefficients that transform a known input model at the survey location to a desired output at the pole. Keating and Zerbo (1996) also used Wiener filtering by introducing a deterministic noise model, allowing the method to be fully automated. Li and Oldenburg (1998b, 2000a) proposed a technique that attempts to find the RTP field under the general framework of an inverse formulation, with the RTP field constructed by solving an inverse problem in which a global objective function is minimized subject to fitting the observed data.

All of these techniques assume that the directions of magnetization and ambient field are invariant over the entire survey area. While this is appropriate for many studies, it is not appropriate for continent-scale studies, over which the earth's magnetic-field direction varies significantly, or in geologic environments, where remanent magnetization is important and variable. Arkani-Hamed (1988) addressed the former problem with an equivalent-layer scheme, in which variations in magnetization and ambient-field directions were treated as perturbations on uniform directions.

Pseudogravity transformation

Poisson's relation shows that gravity and magnetic anomalies caused by a uniformly dense, uniformly magnetized body are related by a first derivative. Baranov (1957) used this principle to transform an observed magnetic anomaly into the gravity anomaly that would be observed if the distribution of magnetization were replaced with a proportional density distribution. Baranov called the transformed data pseudogravity, although the pseudogravity anomaly is equivalent to the magnetic potential. The pseudogravity transformation is most commonly used as an interim step to several other edge-detection or depth-estimation techniques or in comparing with observed gravity anomalies. Since calculation of the pseudogravity anomaly involves a reduction to the pole followed by a vertical integration, it is affected by the same instabilities that were present in calculating the RTP field. In addition, the pseudogravity transformation amplifies long wavelengths, and so grids must be expanded carefully before processing to minimize amplification of long-wavelength noise.

Upward-downward continuation

Magnetic data measured on a given plane can be transformed to data measured at a higher or lower elevation, thus either attenuating or emphasizing shorter wavelength anomalies (Kellogg, 1953). These analytic continuations lead to convolution integrals which can be solved either in the space or frequency domain. The earliest attempts were done in the space domain by deriving a set of weights which, when convolved with field data, yielded approximately the desired transform (Peters, 1949; Henderson, 1960; Byerly, 1965). Fuller (1967) developed a rigorous approach to determining the required weights and analyzing their performance. The space-domain operators were soon replaced by frequency-domain operators. Dean (1958) was the first to recognize the utility of using Fourier transform techniques in performing analytic continuations. Bhattacharyya (1965), Byerly (1965), Mesko (1965), and Clarke (1969) contributed to the understanding of such transforms, which now are carried out on a routine basis. It is worth mentioning that while upward continuation is a very stable process, the opposite is true for downward continuation where special techniques, including filter response tapering and regularization, have to be applied in order to control noise.

Analytic continuations are usually performed from one level surface to another. To overcome this limitation, Syberg (1972b) and Hansen and Miyazaki (1984) extended the

potential-field theory to continuation between arbitrary surfaces, and Parker and Klitgord (1972) used a Schwarz-Christoffel transformation to upward continue uneven profile data. Methods using equivalent sources were proposed by Bhattacharyya and Chan (1977a) and Li and Oldenburg (1999). Techniques designed to approximate the continuation between arbitrary surfaces include the popular chessboard technique (Cordell, 1985a), which calculates the field at successively higher elevations, followed by a vertical interpolation between various strata and a Taylor series expansion (Cordell and Grauch, 1985).

Derivative-based filters

First and second vertical derivatives emphasize shallower anomalies and can be calculated either in the space or frequency domains. These operators also amplify high-frequency noise, and special tapering of the frequency response is usually applied to control this problem. A stable calculation of the first vertical derivative was proposed by Nabighian (1984) using 3D Hilbert transforms in the X and Y directions. Before the digital age, use of the second vertical derivative for delineating and estimating depths to the basement formed the basis of aeromagnetic interpretation (Vacquier et al., 1951; Andreasen and Zietz, 1969).

Many modern methods for edge detection and depth-to-source estimation rely on horizontal and vertical derivatives. Gunn et al. (1996) proposed using vertical gradients of order 1.5 and also showed the first use of complex analytic signal attributes in interpretation. Use of the horizontal gradient for locating the edges of magnetic sources developed as an extension of Cordell's (1979) technique to locate edges of tabular bodies from the steepest gradients of gravity data. Like gravity anomalies, a pseudogravity anomaly has its steepest gradients located approximately over the edges of a tabular body. Thus, Cordell and Grauch (1982, 1985) used crests of the magnitude of the horizontal gradient of the pseudogravity field as an approximate tool for locating the edges of magnetic bodies. In practice, this approach can also be applied to the reduced-to-the-pole magnetic field. This results in improved edge resolution, but some caution is required to avoid misinterpreting low-amplitude gradients attributable to side lobes (Phillips, 2000; Grauch et al., 2001).

Blakely and Simpson (1986) presented a useful method for automatically locating and characterizing the crests of the horizontal gradient magnitude. A method by Pearson (2001) finds breaks in the direction of the horizontal gradient by application of a moving-window artificial-intelligence operator. Another, similar technique is skeletonization (Eaton and Vasudevan, 2004), which produces not only an image but also a database of each lineament element, which can be sorted and decimated by length or azimuth criteria. Thurston and Brown (1994) developed convolution operators for controlling the frequency content of the horizontal derivatives and, thus, of the resulting edges. Cooper and Cowan (2003) introduced the combination of visualization techniques and fractional horizontal gradients to more precisely highlight subtle features of interest.

The main advantages of the horizontal gradient method are its ease of use and stability in the presence of noise (Phillips, 2000; Pilkington and Keating, 2004). Its disadvantages arise when edges are dipping or close together (Grauch and Cordell, 1987; Phillips, 2000) or when assumptions regarding magnetization direction are incorrect during the initial RTP or pseudogravity transformation. The method can also give misleading results when gradients from short-wavelength anomalies are superposed on those from long-wavelength anomalies. To address this problem, Grauch and Johnston (2002) developed a windowed approach to help separate local from regional gradients.

The total gradient (analytic signal) is another popular method for locating the edges of magnetic bodies. For magnetic profile data, the horizontal and vertical derivatives fit naturally into the real and imaginary parts of a complex analytic signal (Nabighian, 1972, 1974, 1984; Craig, 1996). In 2D (Nabighian, 1972), the amplitude of the analytic signal is the same as the total gradient, is independent of the direction of magnetization, and represents the envelope of both the vertical and horizontal derivatives over all possible directions of the earth's field and source magnetization. In 3D, Roest et al. (1992) introduced the total gradient of magnetic data as an extension to the 2D case. Unlike the 2D case, the total gradient in 3D is not independent of the direction of magnetization (Haney et al., 2003), nor does it represent the envelope of both the vertical and horizontal derivatives over all possible directions of the earth's field and source magnetization. Thus, despite its popularity, the total gradient is not the correct amplitude of the analytic signal in 3D. It is worth noting that what is now commonly called analytic signal should correctly be called the total gradient.

The main advantage of the total gradient over the maximum horizontal gradient is its lack of dependence on dip and magnetization direction, at least in 2D. The approaches used to locate magnetic edges using the crests of the horizontal gradient can also be applied to the crests of the total gradient. This difference in the two methods can be used to advantage — differences in edge locations determined by the two techniques can be used to identify the dip direction of contacts (Phillips, 2000) or to identify remanent magnetization (Roest and Pilkington, 1993).

If the total gradient of the magnetic field is somewhat analogous to the instantaneous amplitude used in seismic data analysis, then the local phase, defined as the arctangent of the ratio of the vertical derivative of the magnetic field to the horizontal derivative of the field, is analogous to the instantaneous phase. The local wavenumber, analogous to the instantaneous frequency, is defined as the horizontal derivative in the direction of maximum curvature of the local phase. Thurston and Smith (1997) and Thurston et al. (1999, 2002) showed that the local wavenumber is another function that has maxima over the edges of magnetic sources. Like the total gradient, the local wavenumber places maxima over the edges of isolated sources, regardless of dip, geomagnetic latitude, magnetization direction, or source geometry (see "Magnetic Inverse Modeling" section, "Source parameter imaging" subsection, which follows). The full expression for calculating the 3D local wavenumber is complicated (Huang and Versnel, 2000) and tends to produce noisy results. A better result is achieved by considering only the effects of 2D sources (Phillips, 2000; Pilkington and Keating, 2004).

An alternate function that is easy to compute and approximates the absolute value of the full 3D local wavenumber

is the horizontal gradient magnitude of the tilt angle (Miller and Singh, 1994; Pilkington and Keating, 2004; Verduzco et al., 2004). The tilt angle, first introduced by Miller and Singh (1994), is the ratio of the first vertical derivative to the horizontal gradient and is designed to enhance subtle and prominent features evenly.

Finally, a form of filter that can be used to highlight faults is the Goussev filter, which is the scalar difference between the total gradient and the horizontal gradient (Goussev et al., 2003). This filter, in combination with a depth separation filter (Jacobsen, 1987), provides a different perspective from other filters and helps discriminate between contacts and simple offset faults. Wrench faults show up particularly well as breaks in the linear patterns of a Goussev filter.

Matched filtering

Spector (1968) and Spector and Grant (1970) showed that logarithmic radial-power spectra of gridded magnetic data contain constant-slope segments that can be interpreted as arising from statistical ensembles of sources, or equivalent source layers, at different depths. Spector (1968) designed the first Fourier and convolution filters designed to separate the magnetic anomalies produced at two different source depths. The convolution filter was published by Spector (1971), while the Fourier filter was published, in simplified form, by Spector and Parker (1979). Syberg (1972a) first applied the term *matched filter* to this process of matching the filter parameters to the power spectrum and developed Fourier-domain filters for separating the magnetic field of a thin, shallow layer with azimuthally dependent power from the magnetic field of a deeper magnetic half-space having different azimuthally dependent power. A Fourier filter for extracting the anomaly of the deepest source ensemble, without requiring any estimated parameters for shallow sources, was presented by Cordell (1985b). Ridsdill-Smith (1998a, b) developed wavelet-based matched filters, while Phillips (2001) generalized the Fourier approach of Syberg (1972a) to sources at more than two depths and explained how matched Wiener filters could be used as an alternative to the more common amplitude filters.

An alternative to matched filters, based on differencing of upward continued fields, was developed by Jacobsen (1987). Cowan and Cowan (1993) reviewed separation filtering and compared results of Spector's matched filter, the Cordell filter, the Jacobsen filter, and a second vertical derivative filter on an aeromagnetic data set from Western Australia.

Wavelet transform

The wavelet transform is emerging as an important processing technique in potential-field methods and has contributed significantly to the processing and inversion of both gravity and magnetic data. The concept of continuous wavelet transform was initially introduced in seismic data processing (Goupillaud et al., 1984), while a form of discrete wavelet transform has long been used in communication theory. These were unified through an explosion of theoretical developments in applied mathematics. Potential-field analysis and magnetic methods in particular, have benefited greatly from these developments.

The use of wavelets has been approached in three principle ways. The first approach uses continuous wavelet transforms based on physical wavelets, such as those developed by Moreau et al. (1997) and Hornby et al. (1999). The former analyzes potential-field data using various wavelets derived from a solution of Poisson's equation, while the latter group takes a more intuitive approach and recasts commonly used processing methods in potential fields in terms of continuous wavelet transforms. These wavelets are essentially second-order derivatives of the potential produced by a point monopole source taken in different directions. Methods based on the continuous wavelet transform identify locations and boundaries of causative bodies by tracking the extrema of the transforms. Sailhac et al. (2000) applied a continuous wavelet transform to aeromagnetic profiles to identify source location and boundaries. Haney and Li (2002) developed a method for estimating dip and the magnetization direction of two-dimensional sources by examining the behavior of extrema of continuous wavelet transforms.

A second class of wavelet methodologies utilizes discrete wavelet transforms based on compactly supported orthonormal wavelets. Chapin (1997) applied wavelet transforms to the interpretation of gravity and magnetic profiles. Ridsdill-Smith and Dentith (1999) used wavelet transforms to enhance aeromagnetic data. LeBlanc and Morris (2001) applied discrete wavelet transforms to remove noise from aeromagnetic data. Finally, Vallee et al. (2004) used this method to perform depth estimation and identify source types.

In a third approach, discrete wavelet transforms are used to improve the numerical efficiency of inversion-based techniques. Li and Oldenburg (2003) used discrete wavelet transforms to compress the dense sensitivity matrix in 3D magnetic inversion and thus reduce both memory requirement and CPU time in large-scale 3D inverse problem. A similar approach is also applied to the problem of upward continuation from uneven surfaces (Li and Oldenburg, 1999) and reduction to the pole using equivalent sources (Li and Oldenburg, 2000a).

MAGNETIC FORWARD MODELING

Before the use of electronic computers, magnetic anomalies were interpreted using characteristic curves calculated from simple models (Nettleton, 1942) or by comparison with calculated anomalies over tabular bodies (Vacquier et al., 1951). In the 1960s, computer algorithms became available for calculating magnetic anomalies across two-dimensional bodies of polygonal cross sections (Talwani and Heirtzler, 1964) and over three-dimensional bodies represented by right rectangular prisms (Bott, 1963; Bhattacharyya, 1964), by polygonal faces (Bott, 1963), or by stacked, thin, horizontal sheets of polygonal shape (Talwani, 1965).

The 2D magnetic forward-modeling algorithm of Talwani and Heirtzler (1964) was later modified to include bodies of finite strike length (Shuey and Pasquale, 1973; Rasmussen and Pedersen, 1979; Cady, 1980), referred to as 2 1/2D. Computer programs to calculate magnetic and gravity profiles across these 2 1/2D bodies, and also perform inversions, began to appear in the 1980s (Saltus and Blakely, 1983, 1993; Webring, 1985).

The 3D magnetic forward-modeling algorithm of Talwani (1965) was modified by Plouff (1975, 1976), who replaced the

thin horizontal sheets with finite-thickness prisms. The approach of Bott (1963) to modeling 3D bodies using polygonal facets was also used by Barnett (1976), who used triangular facets, and by Okabe (1979). A subroutine based on Bott's approach appears in Blakely (1995). A complete treatment of gravity and magnetic anomalies of polyhedral bodies can be found in Holstein (2002a, b).

Much attention has been paid to expressions for the Fourier transforms of magnetic fields of simple sources, both as a means of forward modeling and as an aid to inversion (Bhattacharyya, 1966; Spector and Bhattacharyya, 1966; Pedersen, 1978; Blakely, 1995). Parker (1972) presented a practical Fourier method for modeling complex topography, in which the observations are on a flat plane or other surface that is above all the sources. Blakely (1981) published a computer program based on Parker's method, and Blakely and Grauch (1983) used the method to investigate terrain effects in aeromagnetic data flown on a barometric surface over the Cascade Mountains of Oregon.

The venerable right-rectangular prism has remained popular for voxel-based magnetic forward modeling and inversion. Hjelt (1972) presented the equations for the magnetic field of a dipping prism having two opposite vertical sides that are parallelograms. This particular form of the voxel is useful for modeling magnetic anomalies caused by layered strata distorted by geologic processes, such as faulting and folding (Jessell et al., 1993; Jessell and Valenta, 1996; Jessell, 2001; Jessell and Fractal Geophysics, 2002).

MAGNETIC INVERSE MODELING

From a purely mathematical point of view, there is always more than one model that will reproduce the observed data to the same degree of accuracy (the so-called nonuniqueness problem). However, geologic units producing the magnetic data that we acquire in real-world problems do not have an arbitrary variability. Imposing simple restrictions on admissible solutions based on geologic knowledge and integration with other independent data sets and constraints leads usually to distinct and robust results.

Depth-to-source estimation techniques

With the first aeromagnetic surveys came the recognition that the largest magnetic anomalies were produced by sources near the top of the crystalline basement, and that the wavelengths of these anomalies increased as the basement rocks became deeper. Techniques were devised to estimate the depths to the magnetic sources and, thus, the thickness of the overlying sedimentary basins. Mapping basement structure became an important application of the new aeromagnetic method.

Early depth-to-source techniques were mostly of graphical nature and applicable only to single-source anomalies (Henderson and Zietz, 1948; Peters, 1949; Vacquier et al., 1951; Smellie, 1956; Hutchison, 1958; Grant and Martin, 1966; Koulomzine et al., 1970; Barongo, 1985). These techniques estimated target parameters by looking at various attributes of an anomaly (curve matching, straight-slope, half-width, amplitude, horizontal extent between various characteristic points, etc). The straight-slope method in particular enjoyed immense popularity with interpreters working in petroleum exploration. Smith (1959) gave various rules for estimating the maximum possible depth to various magnetic sources. Trial-and-error methods were also developed (Talwani, 1965), in which magnetic anomalies were calculated iteratively until a good fit with observed data was obtained.

In the 1970s, automated depth analysis began to supplant the graphical and trial-and-error techniques. These new methods took advantage of the digital aeromagnetic data that began to appear at that time, and they typically generated large numbers of depth estimates along magnetic profiles based on simple but geologically reasonable 2D models such as sheets, contacts, or polygonal corners. Because validity of the models could not be assumed, the depth estimates still needed to be tested for reasonableness by appropriate forward modeling.

In the 1990s, 3D automated depth-estimation methods began to appear. These were largely extensions of 2D methods designed for application to gridded magnetic data. Most of the methods mentioned below still exist in commercial or public-domain software. There is no best method, and it is wise to use a variety of methods to identify consistent results: forward modeling is still a good idea.

Werner deconvolution

Automated depth-determination techniques have been limited mostly to profile data by assuming that targets are two-dimensional. Werner (1955) proposed a method for interpreting overlapping effects of nearby anomalies if they can be interpreted as attributable to thin sheets. Assuming the causative bodies are two-dimensional and have a polygonal cross section, this can be achieved by taking the horizontal derivative of the observed profile. The method, now known as Werner deconvolution, was first implemented by Hartman et al. (1971) and further refined by Jain (1976), Kilty (1983), Ku and Sharp (1983) and Tsokas and Hansen (1996). The method was first extended to multiple 2D sources by Hansen and Simmonds (1993) and later extended to 3D multiple sources by Hansen (2002). The extension to multiple sources was achieved using deconvolution on the complex form of the analytic signal.

CompuDepth

O'Brien (1972) introduced CompuDepth, a frequency-domain technique that determines location and depth to 2D magnetic sources based on successive frequency shifting of the Fourier spectrum, linear phase filtering, and solving a system of equations for the various target parameters. Wang and Hansen (1990) extended the method of O'Brien to invert for the corners of 3D homogeneous polyhedral bodies.

Naudy method

Naudy (1971) proposed a method that uses a matched filter based on the calculated profile over a vertical dike or thin plate. The filter is applied twice, first to the symmetrical component of the aeromagnetic profile and then to the symmetrical component of the same profile reduced to the pole. Shi (1991) improved convergence of the Naudy method by using horizontal and vertical components of the magnetic profile instead of observed and reduced-to-the-pole components

and also extended the analysis to include dip estimates for the dikes.

Analytic signal

Nabighian (1972, 1974) introduced the concept of the analytic signal for magnetic interpretation and showed that its amplitude yields a bell-shaped function over each corner of a 2D body with polygonal cross section. For an isolated corner, the maximum of the bell-shaped curve is located exactly over the corner, and the width of the curve at half its maximum amplitude equals twice the depth to the corner. The determination of these parameters is not affected by the presence of remanent magnetization. Horizontal locations are usually well determined by this method, but depth determinations are only reliable for polyhedral bodies. Roest et al. (1992) used the total magnetic gradient, which they called the 3D analytic signal to approximately estimate positions of magnetic contacts and obtain some depth estimates from gridded data. Their results, however, are strongly dependent on the direction of total magnetization, in sharp contrast with the 2D case.

Euler deconvolution

Thompson (1982) proposed a technique for analyzing magnetic profiles based on Euler's relation for homogeneous functions. The Euler deconvolution technique uses first-order x, y- and z derivatives to determine location and depth for various idealized targets (sphere, cylinder, thin dike, contact), each characterized by a specific structural index. Although theoretically the technique is applicable only to a few body types which have a known constant structural index, the method is applicable in principle to all body types. Reid et al. (1990) extended the technique to 3D data by applying the Euler operator to windows of gridded data sets. Mushayandebvu et al. (2000) and Silva and Barbosa (2003), among others, helped in understanding the applicability of the technique. Mushayandebvu et al. (2001) introduced a second equation derived from Euler's homogeneity equation which, when used in conjunction with the standard Euler equation, led to more stable solutions. This technique is now known as extended Euler deconvolution. The extended Euler deconvolution technique was generalized to 3D by Nabighian and Hansen (2001) using generalized Hilbert transforms (Nabighian, 1984). In the same paper, the authors showed that their proposed technique is also a 3D generalization of the Werner deconvolution technique, and thus both can be presented under a single unified theory. Although Barbosa et al. (1999) showed that attempting joint estimation of depth and structural index leads to unstable results using the traditional least-squares approach, others have claimed success by using alternative approaches such as differential similarity transformations (Stavrev, 1997; Gerovska and Araúzo-Bravo, 2003) and generalized Hilbert transform (Nabighian and Hansen, 2001; Fitzgerald et al., 2003). Hansen and Suciu (2002) extended the single-source Euler deconvolution technique to multiple sources to better account for the overlapping effects of nearby anomalies. Keating and Pilkington (2000) and Salem and Ravat (2003) proposed applying Euler deconvolution to the amplitude of the analytic signal, while Zhang et al. (2000) showed how the technique could be applied to tensor data. Phillips (2002) proposed a two-step methodology for 3D magnetic source locations and structural indices using extended Euler or analytic signal methods. Finally, Mushayandebvu et al. (2004) showed that eigenvalues generated in the grid Euler solution could be exploited to decide automatically whether an individual anomaly was 2D or 3D and, in the former case, could be exploited to deduce strike and dip.

Source parameter imaging (SPI™)

Thurston and Smith (1997) and Thurston et al. (1999, 2002) developed the source parameter imaging (SPI) technique, based on the complex analytic signal, which computes source parameters from gridded magnetic data. The technique is sometimes referred to as the local wavenumber method. The local wavenumber has maxima located over isolated contacts, and depths can be estimated without assumptions about the thickness of the source bodies (Smith et al., 1998). Solution grids using the SPI technique show the edge locations, depths, dips and susceptibility contrasts. The local wavenumber map more closely resembles geology than either the magnetic map or its derivatives. The technique works best for isolated 2D sources such as contacts, thin sheet edges, or horizontal cylinders.

The SPI method requires first- and second-order derivatives and is thus susceptible to both noise in the data and to interference effects. Phillips (2000) compared the SPI method with the total-horizontal-gradient and analytic-signal methods and showed how the methods differ in their assumptions, accuracy, and sensitivity to noise and anomaly interference.

Statistical methods

All of the above techniques attempt to determine the location, shape, and depth of specific isolated targets. An entirely different approach considers the anomaly to be caused by an ensemble of magnetic sources in order to determine their average depth. The method was first proposed by Spector and Grant (1970) and further refined by Treitel et al. (1971). Their method assumes that parameters of individual sources (length, width, depth, etc.) are governed by probabilities. Spector and Grant (1970) showed that the spectral properties of an ensemble of sources is equivalent to the spectral properties of an average member of the ensemble. For a single ensemble, the natural log of the radial power density spectrum as a function of wavenumber will have a linear slope approximately twice the maximum depth of the ensemble. For multiple ensembles, one obtains linear slopes approximately twice the maximum depths to the various magnetic ensembles. More accurate depths can be estimated by progressively stripping off effects of the shallowest ensembles (or equivalent layers), and by correcting the power spectrum for source body width (Spector and Grant, 1970, 1974) or for fractal magnetization models (Pilkington et al., 1994). The last approach was further expanded by Maus (1999) and Maus et al. (1999) as a robust method for depth-to-basement calculations. Computer programs for source depth estimation from magnetic profiles using windowed statistical approaches were published by Phillips (1979) and Blakely and Hassanzadeh (1981).

Physical Property Mapping

Terracing

Terracing (Cordell and McCafferty, 1989) is an iterative filtering method applied to gridded magnetic (or gravity) data that gradually increases the slopes of the first horizontal derivatives while simultaneously flattening the field between gradients. The resulting map is similar to a terraced landscape, hence the name applied to this technique. When imaged as a color map and illuminated from above, a terraced map resembles a geologic map in which the color scheme approximates the relative magnetizations of the geologic units. The method can be further refined by assigning susceptibility values to each unit by least-squares approximations until the calculated field agrees reasonably well with the measured data.

Susceptibility mapping

Grant (1973) introduced a special form of inversion in which gridded magnetic data are inverted in the frequency domain to provide the apparent magnetic susceptibility of a basement represented by a large number of infinite vertical prisms. The maps thus obtained reflect the geology of the area, insofar as susceptibility is related to rock type. A similar approach was applied to the inversion of marine magnetic anomalies in 2D (Parker and Huestis, 1974) and 3D (Macdonald et al., 1980). Analogous space-domain methods were developed by Bhattacharyya and Chan (1977b), Silva and Hohmann (1984), and Misener et al. (1984) by reducing the problem to solving a large system of equations relating the observed data to magnetic sources in the ground.

Inversion

Inversion refers to an automated numerical procedure that constructs a model of subsurface geology from measured magnetic data and any prior information, with the additional condition that the input data are reproduced within a given error tolerance. Quantitative interpretation is then carried out by drawing geologic conclusions from the inverted models.

As is typical for geophysical inverse problems, a purely mathematical solution of magnetic inversion is nonunique. The nonuniqueness arises mainly for two reasons. First, there are only a finite number of inaccurate measurements. Consequently, there is always more than one model that will reproduce the observed data to the same degree of accuracy. Second, Green's theorems dictate that many subsurface distributions of magnetization can produce exactly the same surface response. It is therefore important to recognize that even though magnetic inversion is nonunique from a purely mathematical point of view, it is equally important to understand that the often overemphasized nonuniqueness stems mainly from the mathematical properties of potential fields and has little to do with realistic geologic scenarios. In reality, geologic units producing the magnetic data that we acquire in real-world problems do not have an arbitrary variability. Imposing simple restrictions on admissible solutions based on geologic knowledge and integration with other independent data sets and constraints usually leads to distinct and robust results.

In inversion methodology, a model is parameterized to describe either source geometry or the distribution of a physical property such as magnetic susceptibility. These lead to two major approaches to magnetic inversion.

The first approach inverts for the geometry of the source distribution. For example, following Bott's (1960) work on inverting gravity data for basin depth by iteratively adjusting the depth of vertical prisms, several authors have formulated depth-to-basement inversion in a similar manner (e.g., Pedersen, 1977). Pilkington and Crossley (1986) inverted magnetic anomalies to estimate basement relief by applying linear inverse theory and Parker's (1972) forward-calculation technique. Pustisek (1990) developed a noniterative procedure to invert for magnetic basement.

For isolated anomalies, the first attempts parameterized the causative body with a single dike in 2D and rectangular prism in 3D. A parametric inversion was then carried out to recover the target parameters through the use of nonlinear least squares (e.g., Whitehill, 1973; Ballantyne, 1980; Bhattacharyya, 1980; and Silva and Homann, 1983). Alternatively, causative bodies are represented as polygonal bodies in 2D or polyhydronal bodies in 3D (Pedersen, 1979; Wang and Hansen, 1990), and the vertices of the objects are recovered as the unknowns.

The second approach inverts for either magnetic susceptibility or magnetization. Parker and Huestis (1974) in their crustal studies inverted for the distribution of magnetization in a layer. Cribb (1976) represented the magnetic source by a set of dipoles and attempted to recover the dipole strengths by applying linear inverse theory. Guillen and Menichetti (1984) used a prismatic representation and performed a regularized inversion by minimizing the moment of inertia of the causative body. Li and Oldenburg (1996) formulated a generalized 3D inversion of magnetic data by using the Tikhonov regularization and a model objective function that measures the structural complexity of the model and incorporates a depth-weighting function. A positivity constraint was also imposed on the recovered density contrast to further stabilize the solution. Pilkington (1997) introduced acceleration to this method by using the conjugate gradient. Li and Oldenburg (2000b, 2003) extended the method to include borehole data and applied wavelet-compression-based acceleration and a logarithmic method for imposing positivity.

Most of these methods assume that the magnetization direction is known. As a result, their application is limited when strong remanent magnetization alters the total magnetization direction. To overcome this difficulty, Shearer and Li (2004) developed a 3D nonlinear inversion to recover the magnetization magnitude by inverting the amplitude of the anomalous magnetic vector or the total gradient of the magnetic anomaly. These two quantities exhibit weak dependence on the direction of magnetization; therefore, precise knowledge of the latter is not required.

GEOLOGIC INTERPRETATION OF MAGNETIC DATA

Magnetic data, processing, and analysis give information and constraints about the distribution of magnetic materials at the surface and below. The goal of geologic interpretation is to render this information into a model of salient geologic features where they are not exposed. Modern geologic interpretation involves a complex synthesis of multiple aspects: the results of magnetic analysis, geologic knowledge of the study

area, an understanding of rock-magnetic properties, integration with other independent data sets and constraints, geologic characterization of anomaly shapes and patterns, and identification of the contributions of topography and cultural sources. Over the past 75 years, the most significant improvements in the quality and reliability of geologic interpretation have followed from increased data resolution, concurrent advancements in our understanding of all the aspects of the synthesis, and improvements to the processes used to synthesize them (e.g., modeling/inversion, data presentation, and data integration). These advances have continually improved our ability to constrain nonunique results predicted by theory, allowing for solutions that are distinct and robust in practice (see discussions in Gibson and Millegan, 1998, p. 6–8).

Magnetic basement mapping

Shortly after World War II, when the antisubmarine warfare magnetometer was converted to use in geophysical airborne surveys, a new era in oil and gas exploration was born [along with a number of new aeromagnetic companies: AeroService, Fairchild, Compagnie Générale de Géophysique (CGG), Airmag, and Hunting]. The principal product of this flourishing activity was the magnetic basement map interpretation, as described by Steenland (1998).

Steenland's interpretations, when coupled with an understanding of the local and regional geology, were intended as a basis for determining economic basement and (where it was deemed warranted) sedimentary structures controlled by local basement structures. The first step in generating magnetic basement maps was to determine the depths to magnetic sources. He and others favored the straight-slope method, which grew out of the model anomalies comprehensively produced by Vacquier et al. (1951). Because they relied on human computers and were required to interpret very large volumes of aeromagnetic data, many interpreters of that era used this method to such an extent that it dominated the magnetic basement mapping industry. Based on simplicity and speed of calculation, the horizontal distance between points of departure of the magnetic trace from a coincident straight edge (corrected for azimuth) formed the basis for determining depth to basement. Steenland (1963a) gave a description of this technique and a comparison between the magnetic depth estimates and drilling results in the Peace River Arch in western Canada, and his statistical estimates of depth accuracy are still valid. At that time, the only model used was the so-called intrabasement model, believed to be zones of higher magnetic susceptibilities occurring within the basement rocks having great depth extent. At about the same time, but too late to incorporate in the Peace River publication, the suprabasement (or thin-plate) model was introduced, together with new indices for adjusting the derived depths. This model is included in a study of the Paradox Basin, Utah, together with a discussion of several aeromagnetic products that were generated in the 1960s and later (Steenland, 1962).

Steenland (1963a) did not argue that the straight-slope method is the most accurate method; he and others favored it for economic reasons. But they did insist (Nettleton, 1971, p. 98) that this method particularly, and the aeromagnetic method generally, produced consistently accurate depth-to-basement maps. Not all agreed. Jacobsen (1961, p. 316) published an interesting blind test, in which two contractors had submitted interpretations of an aeromagnetic survey in Venezuela: "Local basement relief shown by the two magnetic interpretations is in poor agreement with basement depth information from seismograph and well data. Moreover, the two magnetic pictures bear little resemblance one to the other." However, in a discussion of this paper [R. J. Bean of Shell (Bean et al., 1961, p. 317)] commented that "One of the contour maps (Interpretation A) is excellent" and that "any magnetic interpreter would be extremely gratified if all his basement contour maps checked as well as this one with data obtained subsequently by seismic surveys or by drilling." Interestingly, Steenland (who did not comment at the time because he was the Editor of (GEOPHYSICS) later (1963b) revealed that he was the author of Interpretation A.

Geologic characterization of magnetic anomalies

Recognition of characteristic patterns and shapes of anomalies in relation to particular rock units or geologic structures is one of the first steps in qualitative interpretation of a magnetic map. Correlation of magnetic maps to exposed geologic units was well established over 75 years ago (Stearn, 1929a). The correlation involves recognition of anomaly patterns typical of certain rock types or units particular to a study area, identification of breaks in anomaly patterns that may indicate structures, and delineating linear gradients. Seeing changes in anomaly patterns can be subjective and interpreted as differences in terranes, lithologies, or alteration.

With the advent of HRAM surveys, many near-surface geologic features are so clearly expressed that their geologic origin is obvious in color shaded-relief images. For example, dendritic patterns of modern channels and paleochannels or glacial till are mimicked in the aeromagnetic data (Figure 1; Gunn, 1997; Davies et al., 2004; Gay, 2004). Folds look like folds (Figure 1); fault expressions can exhibit en echelon and anastomosing behavior (Figure 2; Grauch et al., 2001; Langenheim et al., 2004); and individual dikes within swarms are clearly resolved (Hildenbrand and Raines, 1990; Modisi et al., 2000). Within sedimentary basins, HRAM surveys allow a clear distinction between basement anomalies and near-surface volcanic rocks and between basement faults and near-surface faults (southwest corner of Figure 2). Volcanic rocks are typically associated with characteristic high-frequency patterns, which can be differentiated from circular and sometimes broader anomalies associated with intrusions (Figure 2). Magnetic anomalies produced by rocks with strong, reverse-polarity remanence display characteristic, high-amplitude negative anomalies (south-central border of Figure 2; Books, 1962; Grauch et al., 1999) that, without high-resolution data, might be confused with magnetic lows caused by a lack of magnetization, which are also negative but generally featureless (Airo, 2002). The featureless character is well demonstrated in the HRAM image from the Murray Basin (Figure 1), where the underlying interpreted granite was confirmed by drilling (Bush et al., 1995).

DATA INTEGRATION / PRESENTATION

Some of the most profound improvements in geologic interpretation over the past 75 years have occurred in the realm of data presentation and integration with other data sets.

Visualization is key to understanding the patterns in data and how they interact with independent data sets.

Although magnetic data were acquired along grid-like traverses or parallel lines as early as the late 19th century, the data were usually displayed in profile form (Smock, 1876; Smyth, 1896). By the 1920s, contour maps were a common way to display magnetic measurements (Stearn, 1929b; Heiland and Courtier, 1929). Contour maps of magnetic field intensity became the primary display for magnetic maps for decades afterward, surviving the analog to digital transition of the 1970s through the development of automated contouring programs. Automated color-filled contour maps made their debut in the early 1980s, which facilitated the assessment of regional trends and magnitude variations (Paterson and Reeves, 1985). The volume, *The Utility of Regional Gravity and Magnetic Maps*, edited by Hinze (1985b), was one of the first SEG publications to rely extensively on color contour maps. By the late 1980s, magnetic interpreters were borrowing from remote-sensing imaging technologies in the form of gray and color gradational images and shaded-relief images (Cordell and Knepper, 1987). By the mid-1990s, the color shaded-relief display was in common use. Today, many of these algorithms allow real-time variation of sun angle and 3D perspective. The shaded-relief display highlights fault zones, dikes, and other semilinear features that are difficult to see in contour-type displays. Complex geology with overlapping anomalies arising from different depths can limit the effectiveness of automated methods, such as fault detection. Sometimes subtle contiguous faults show up better using shaded-relief imaging. However, because a given sun direction highlights features that strike perpendicular to it, it is important to generate enough images with varying sun angles to illuminate all azimuths of lineament/fault trends. Pearson (2001) developed a way to use color to display 24 different sun angles at once.

The Geographic Information System (GIS) revolution in the last decade allows unprecedented digital blending of magnetic anomalies with independent vector and raster information, such as remote sensing images, digital elevation models, electromagnetic data, gamma-ray data, and gravity data. 3D displays can combine any imaginable type of data, including seismic sections, drillhole data, and interpretive results. For example, the magnetic fault identification cube (MaFIC, Rhodes and Peirce, 1999) allows magnetic depth solutions to be integrated with seismic, well, topographic, and filtered magnetic data on any seismic work station.

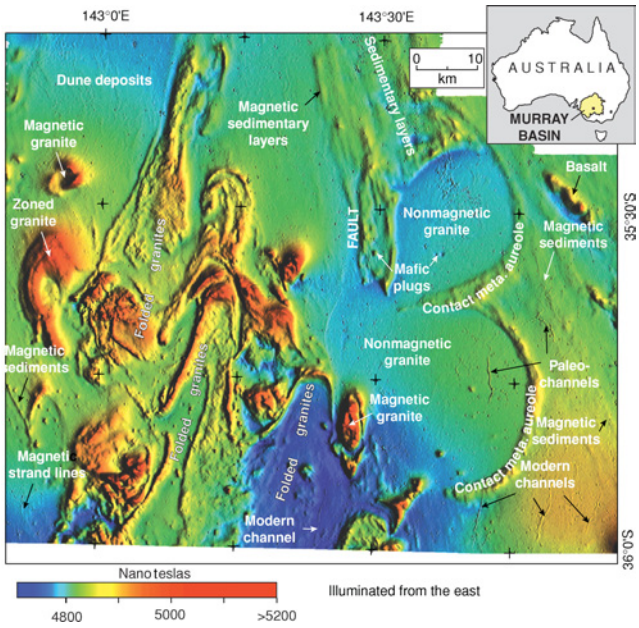

Figure 1. Aeromagnetic data from a portion of the heavy-mineral sand province in the Murray Basin, the region draining into the Murray River in southeastern Australia. The area is almost entirely covered by Quaternary-Tertiary alluvium. Many deposits of the mineral sands produce subtle magnetic anomalies (labeled as magnetic strand lines) but are difficult to see at this regional scale. More obvious are the expressions of a wide variety of other geologic features, as labeled (from interpretations by Bush et al., 1995 and Moore, 2005). The image is derived from data that are ©State of Victoria, Australia, 1999.

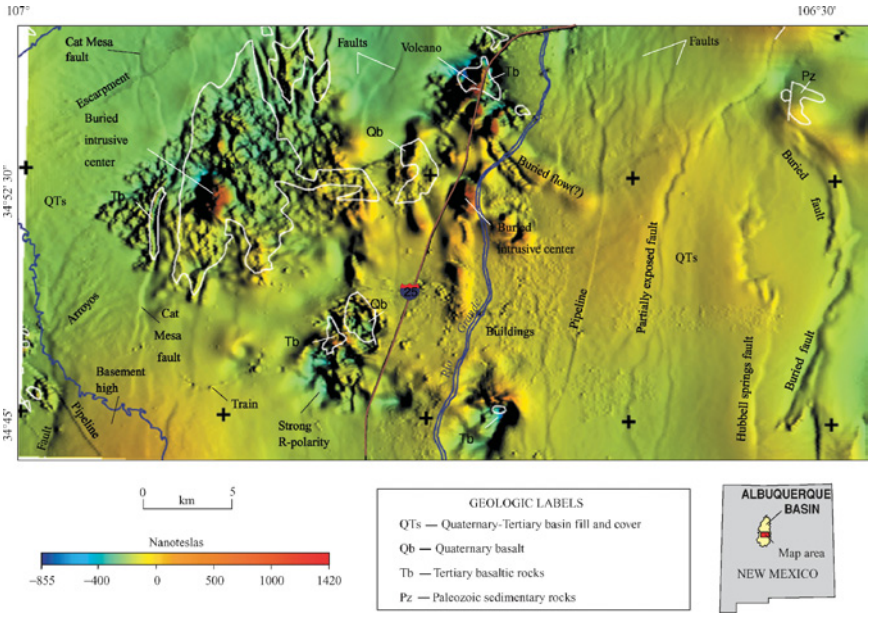

Figure 2. Color shaded-relief image of HRAM data extracted from Sweeney et al. (2002) for a strip crossing the Albuquerque basin just south of the metropolitan area. Geologic contacts (white lines) outline bedrock areas. Intrabasin faults and buried volcanic rocks, which are important for understanding the hydrogeology, are clearly imaged in the HRAM data. The magnetic expressions of the faults commonly connect isolated exposures, which significantly increase the knowledge of their linear extents, patterns, and density. Interstate 25 (brown) and the Rio Grande (dark blue) are labeled.

CASE HISTORIES

Murray Basin, Australia

The Murray Basin, in southeastern Australia, has become a major exploration target for deposits of heavy mineral sands, in large part due to a program of the Victorian government that began to provide high-resolution airborne geophysical data

to the exploration industry in 1994 (www.dpi.vic.gov.au). Heavy mineral sands, which provide titanium and other industrial minerals, are associated with strand lines of Pliocene beach deposits (Roy et al., 2000). They have a weak but discernable signature in airborne magnetic data (Bush et al., 1995).

An example of the Victorian aeromagnetic data, which were acquired at 80 m above ground along lines spaced 250 m apart, is shown in Figure 1. The area is almost entirely devoid of bedrock exposures and the sands are commonly buried under several tens of meters of alluvium as well. Despite this extensive cover, the aeromagnetic image shows not only the subtle features related to heavy mineral sands, but also reveals an amazing variety of geologic features and rock types that reflect the underlying pre-Tertiary rocks (Bush et al., 1995; Moore, 2005). The wide range of geologic sources include magnetic intrusive, volcanic, and sedimentary rocks; nonmagnetic granites surrounded by magnetic, contact metamorphic aureoles; heavy mineral sands in beach deposits; and magnetite and maghemite concentrated in paleochannels. Prominent fold patterns in the western half of the map are accentuated by interlayered magnetic and nonmagnetic granites. Although heavy mineral sands are the focus of exploration in this area, the incredible view into the subsurface that the survey provides demonstrates the utility of aeromagnetic methods for cost effectively mapping the regional geology under cover.

Albuquerque Basin, New Mexico

The Albuquerque basin, part of the Rio Grande rift in north-central New Mexico, not only is a target for oil and gas exploration (e.g., Johnson et al., 2001), but also hosts basin aquifers that are the primary source of water for nonagricultural uses (Bartolino and Cole, 2002). Driven primarily by the increased water demands of a burgeoning population, HRAM surveys (with line spacings and terrain clearances of 100–150 m) were flown over the area in the late 1990s to map buried hydrogeologic features (Grauch et al., 2001). The resulting maps showed intrabasin faults and buried igneous rocks in incredible detail. An example is shown in Figure 2. Both these geologic features can significantly influence groundwater flow paths, rates, and storage.

Figure 2 is extracted from the HRAM data for a strip crossing the basin just south of the Albuquerque metropolitan area. Intrabasin faults appear as widespread, semilinear, shaded anomalies. Exposed basalt fields (labeled as Qb and Tb) correspond to characteristic high-frequency anomaly patterns. The anomaly patterns outside the exposed fields show where volcanic rocks are concealed. Volcanic centers in the southern part of the area produce high-amplitude negative anomalies (area labeled "strong R-polarity" in Figure 2), a signature that is typical of volcanic rocks with strong, reversed-polarity remanent magnetization.

The results from the Albuquerque HRAM survey have implications not only for groundwater exploration but for petroleum exploration as well. First, the magnetic anomalies at the faults can be entirely explained by the tectonic juxtaposition of sediments with differing magnetic properties, despite apparent magnetic lows over the fault zone (Grauch et al., 2001). This result revised a commonly held belief that all such anomalies were caused by alteration or mineralization along the fault plane related to the introduction of hydrocarbon-related fluids. Second, the magnetic images show that the density and linear extent of intrabasin faults are much greater than previously known (Figure 2). Thus, ideas need to be revised concerning the structural style and amount of extension for this and perhaps other basins. Finally, locations of shallow intrabasin faults can be compared to those of deeper basement faults (such as the intrabasin fault located next to the basement high in the southwest corner of Figure 2). The comparison can aid in correlating faults between seismic lines or in developing an understanding of how basement faults propagate to the surface.

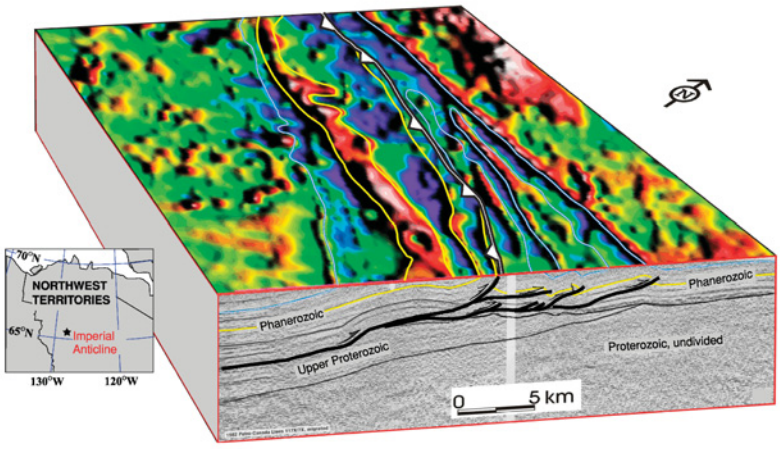

Figure 3. Block diagram illustrating the relationship between thrust structures and residual magnetic anomalies over part of the Imperial Anticline, Northwestern Territories, Canada. The surface panel shows an image from aeromagnetic data collected by the Geological Survey of Canada (Geological Survey of Canada, 2005). Magnetic anomalies clearly correlate with steeply dipping stratigraphy in the hanging wall of the thrust fault, as identified by seismic-reflection data (MacLean and Cook, 2002), shown in the cross-sectional view. Example compiled by Jim Davies, Image Interpretation Technologies, Inc.

Imperial Anticline, Northwest Territories, Canada

The Imperial Anticline is part of a regional thrust system in the northern part of the Canadian Cordillera, Northwest Territories. Although hydrocarbon exploration in the area has waned since the 1980s, the structural setting is similar to those of many other thrust structure plays in the western Cordillera. The regional thrust packages are composed of Phanerozoic and upper Proterozoic sedimentary rocks that were folded and thrust during Laramide time over a regionally thick (up to 14 km) sequence of Proterozoic sedimentary rocks (Cook and MacLean, 2004). Seismic data indicate that the Imperial Anticline formed above a structurally complex, bedding-parallel thrust ramp (Cook and MacLean, 1999).

Aeromagnetic data together with seismic reflection data provide a comprehensive 3D view of the complex structure within the Imperial Anticline (Figure 3). Phanerozoic strata

involved in thrusting, shown in seismic reflection data (MacLean and Cook, 2002), can be correlated to subtle magnetic anomalies in an aeromagnetic survey flown at 200-m mean terrain clearance at 800-m line spacing (Geological Survey of Canada, 2005). After removing a smoothed version of the gridded data from the observed grid, the residual magnetic anomalies (~3 nT amplitude) correlate to two separate magnetic horizons within the Phanerozoic stratigraphy. The anomalies may be produced by magnetic contrasts between shale and carbonate lithologies juxtaposed on one another through deposition. The seismic data show the structural complexities in cross section, whereas the aeromagnetic map displays the lateral extent and orientation of the strata that compose the larger structure.

Raglan deposit, northern Quebec, Canada

The Raglan deposit is located in northern Quebec, Canada, and its nickel mineralization is hosted in ultramafic flow units. Little surface geologic expression is available, and exploration has relied primarily on geophysical studies, in particular magnetic surveys. Total-field magnetic data in the area is typified by seemingly isolated magnetic highs interconnected by arc-like low intensity anomalies. Total-field-intensity magnetic data covering an area of 4 km by 4 km is shown in Figure 4a. Two regions of high magnetic-field intensity are observed, and they correspond to highly magnetic ultramafic outcrops, which contain economic-grade ores. The geologic question was whether the outcrops were associated with a single flow unit or whether they were isolated bodies. The answer had important implications; in the former scenario, it meant that there is great potential for extending the ore reserves beyond that known from the shallower, isolated deposits. To answer this question the data was interpreted using generalized 3D inversion (Watts, 1997; Oldenburg et al., 1998).

For the 3D inversion, the earth below the survey area was represented with 16 000 cubic cells (40 by 40 by 10 cells), each cell having dimensions of 100 m. The inversion was formulated to construct a susceptibility distribution that is smooth in all three spatial directions and close to a zero background,

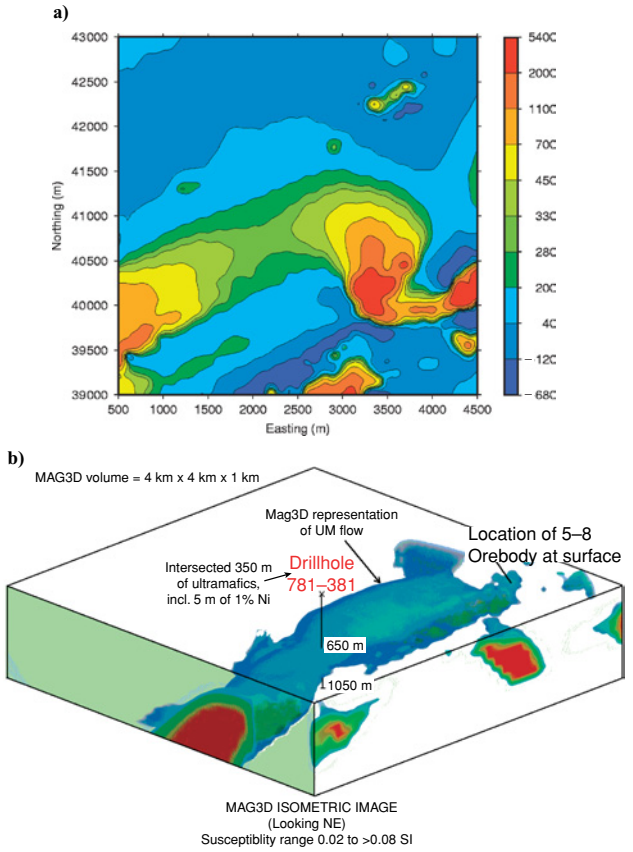

Figure 4. (a) Total field aeromagnetic data. The parameters of the inducing field are I = 83° and D = −32°. Data are contoured in nT. (b) The 3D susceptibility model recovered from magnetic inversion at Raglan deposit. This is a volume-rendered image of the inverted susceptibility model, and the displayed surface provides a representation of the ultramafic flow. Indicated in the volume-rendered representation is the intersecting drill hole that was spotted based upon the inversion results. Darker red colors indicate higher susceptibilities.

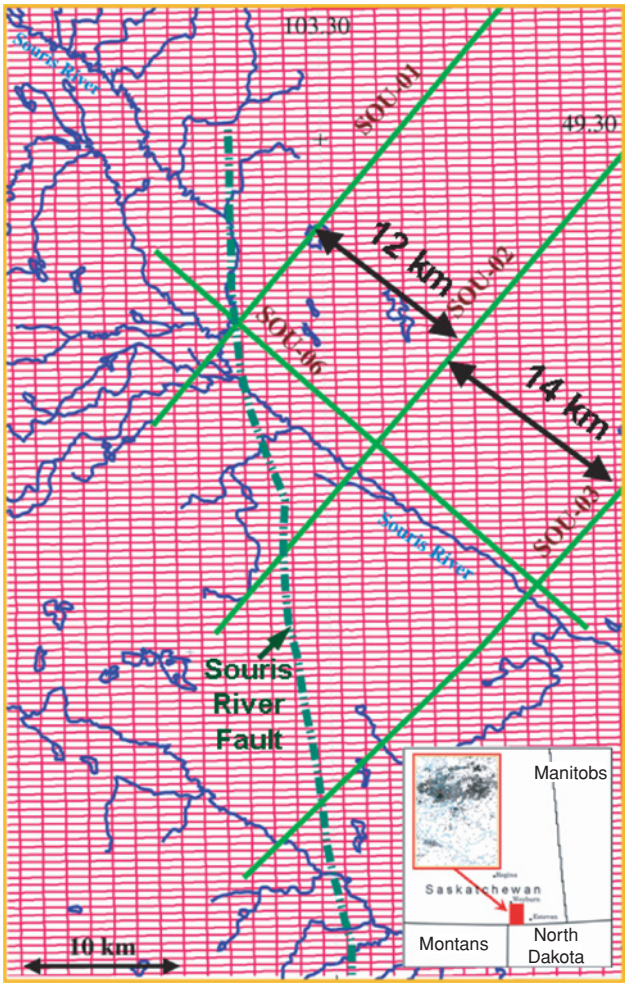

Figure 5. Index map for project showing the use of enhanced HRAM anomalies to correlate faults on 2D seismic data. This example was completed as part of the IEA Weyburn CO_2 Sequestration Project. The study area is shown in red in the inset. The inner inset shows the distribution of wells in the area, including the Weyburn Field. Red lines show the HRAM data (500 × 1500-m line spacing) and the light green lines show the 2D seismic data being correlated. The drainage is shown in blue and the interpreted Souris River Fault is shown as a dark green dashed line.

since the host rocks are, in general, nonmagnetic. The inversion indicated the presence of a continuous zone of highly magnetic material that extended between the two outcrops. The zone is shown as a volume-rendered image (Figure 4b) generated by displaying only susceptibility values greater than 0.04 SI. Ultramafic flows are the only magnetic rocks in the area, so it seemed likely that the highly magnetic region found at depth has the same lithology as that of known deposits. A deep 1100-m hole, sited on the basis of this image, intersected magnetic rocks at a depth of 650 m. Moreover, a 10-m mineralized section (sub-ore grade, approximately 1% nickel) was intersected within the 350-m-thick intersection of magnetic ultramafic rocks. Subsequently, 3D inversion has been used extensively in this region, and new geologic horizons and economic reserves have been found as a direct consequence (A. Watts, personal communication, 1966).

IEA Weyburn CO_2 Sequestration Project, Saskatchewan, Canada

In the IEA Weyburn CO_2 Sequestration Project (Figure 5; Goussev et al., 2004; Wilson and Monea, 2004) a large amount of 2D seismic data was made available to the project for mapping regional-scale faults in the area. The purpose of the mapping was to assess the security of the earth as a container for injected CO_2 gas. The concern about leakage relates to some impurities in the injected gas that would be detrimental to the environment if they leaked to the surface.

Because the faulting patterns were somewhat complicated and the seismic data were relatively widely spaced (Figure 5), Goussev et al. (2004) used GEDCO's proprietary HRAM data as an additional constraint to resolve the spatial aliasing of the fault correlations. Figure 6 shows three seismic lines and one filtered version of the magnetic data. At least six faults are imaged on these three seismic lines, and there is no straightforward correlation of the faults between the lines. The situation is further complicated because the seismic expression of the faults varies from line to line. Using the HRAM data, as enhanced by the Goussev filter, the preferred correlation is shown on the right-hand map of Figure 6, with Fault A being the same on all three seismic images and following the distinct magnetic signature of the fault. This previously unknown fault is now called the Souris River Fault because it offsets the flow of the Souris River from its southeasterly regional flow into a short southerly leg for about 10 km. The fault is clearly present at the basement level on depth-migrated seismic processing, and it penetrates through the entire section to the surface, as evidenced by the course of the Souris River.

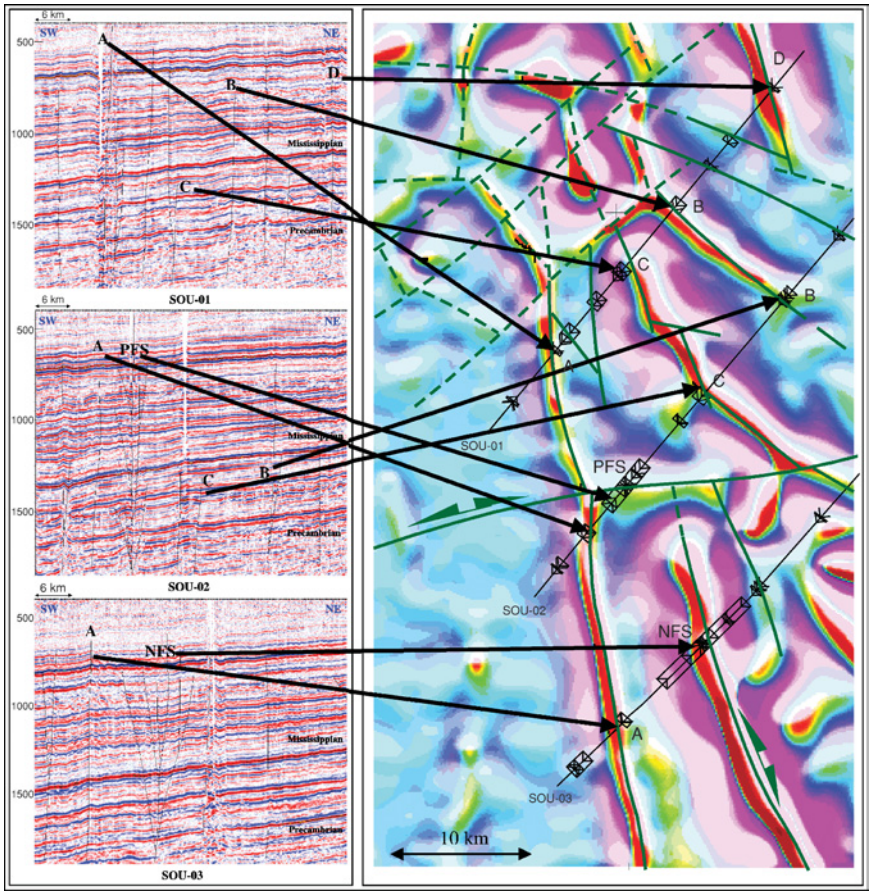

Figure 6. The map on the right shows a Goussev filter of the HRAM data (reds are highs and magenta colors are lows) from the IEA Weyburn CO_2 Sequestration Project. The four seismic lines are shown in dark brown and the fault locations as picked on a seismic workstation are indicated. Panels of seismic lines SOU-1, 2, and 3 are shown on the left, with interpreted faults labeled by letters A-D and PFS (positive flower structure) and NFS (negative flower structure). The positions of those faults on the map are connected to the seismic images of the faults by the yellow arrows. Because the seismic character of the faults is so variable, it is unlikely that anyone would correlate fault A across all three lines with the HRAM data as an additional constraint. Goussev et al. (2004) name this fault the Souris River Fault because it offsets the course of the Souris River into a north-south direction for about 10 km. This fault offsets basement and penetrates to the surface, so it is an important consideration in the IEA Weyburn CO_2 Sequestration Project.

In addition to demonstrating the utility of using HRAM data to constrain ambiguous seismic interpretations, this project also demonstrates clearly that some basement faults penetrate throughout the section in southeastern Saskatchewan. This is an important finding for the IEA CO_2 Sequestration Project. Although there is no evidence that this fault is a leakage path from the reservoir to the surface, the possibility of other basement-to-surface faults exists, and each must be tested for gas leakage to ensure the integrity of the reservoir as a long-term storage container.

LOOKING FORWARD

It seems likely that in the near term, we will see continuing improvements in optically pumped magnetometers. Resolution in the picotesla range and sample rates of around 1 kHz both seem achievable, and various applications could benefit from that

instrument performance. The longer term is as always more difficult to predict. The design of magnetometers has seemed to be a mature science for many decades now, yet there have been order of magnitude improvements in performance over the past 20 years. Perhaps the next 20 will be just as interesting.

We can expect to see a big boom in "boutique" data acquisition systems, such as autonomous and tethered remotely operated vehicles in the deep sea, helicopters carrying multiple sensors, and unmanned drones. Continentwide aeromagnetic data collection could be done almost entirely with drones using a long-lasting power source and cruise missile technology, collecting data 24/7 at very tight line spacing and low terrain clearance over unpopulated areas.

Improvements in GPS will allow exact x, y, and z knowledge of sensor location. Tie-lines will no longer be required because equivalent source technology (or similar methods) will be able to process data directly where collected.

Magnetic gradiometer measurements will be used more commonly as we turn our exploration focus from hydrocarbons and minerals to groundwater. The use of low-flying drones and very accurate GPS will allow us to measure gradient signatures in the uppermost 1000 m of the sedimentary section very accurately. We will need to improve our understanding of what makes sedimentary rocks and unconsolidated sediments magnetic in order to make better interpretations for groundwater exploration and fracture identification.

Aeromagnetic surveys with tighter line spacing will yield information about intrasedimentary lithology, mineralized faults, and geochemical alteration in reconnaissance areas. Aeromagnetic modeling of 3D volumes will proliferate into the hands of more explorationists thanks to competition between software companies. More prolific modeling will yield a better understanding of cultural noise, deep regional noise, and, therefore, exploration targets.

Laboratory measurements of remanent magnetization will discover why 2D and 3D models typically underestimate the amplitude of the observed magnetic field.

Magnetic Curie isotherm and upper-crustal intrusion studies, bolstered by geothermal measurements, will point to prospective areas of basin-centered gas generation.

Spectral decomposition filtering, possibly in the form of matched Wiener models, will assist the Werner and Euler depth techniques at mapping edges within the vertical geologic column. Filters will be developed that will improve our ability to discriminate sources at different depths.

Loading all magnetic data and depth solutions onto a seismic workstation will become standard practice.

ACKNOWLEDGMENTS

The authors wish to sincerely thank Jim Davies for supplying images and information on the Imperial Valley Anticline case history and to David Moore for providing updates and advice on the Murray Basin case history. The manuscript benefited greatly from thoughtful reviews by Rick Blakely, Carol Finn, Peter Gunn, and Alan Reid. Valuable insight on data presentation/integration was provided by William Pearson.

The authors made a serious effort to include in this paper all pertinent developments and references related to the historical development of the magnetic method. In a paper of this magnitude it is inevitable that we might have missed some. This was not intentional and we apologize for any unintended omissions.

APPENDIX A

TIMELINE FOR MAGNETIC METHODS OF EXPLORATION

Date	Event
600 B.C.E.	Thales — Magnetic forces of lodestones
1600	Sir William Gilbert publishes *De Magnete*
1640	Iron ore prospecting begins in Sweden
1840	Carl Friedrich Gauss — Spherical harmonic analysis of geomagnetic data
1850	The first dip needle (Swedish Mining Compass) is developed
1850–1890	Dip needles used primarily as divining rods to prospect for iron ore
1880	Development of earth inductors for magnetic field component measurements
1890–1900	Use of dip needle expands to map iron formations under cover
1896	H. L. Smyth develops magnetic calculations for tabular bodies
1900–1930	Applications expand to include exploration for base metals, oil, and gold
1910	Edelmann — First airborne measurement in balloon
1915	Adolph Schmidt develops vertical field balance
1925-1930	Rock magnetic properties are first studied for interpreting magnetic surveys
1929	Matayama proposes that the earth's magnetic field has experienced reversals
1931	Development of fluxgate magnetometer
1941	Vacquier et al. develop airborne detection of submarines during World War II
1942	Nettleton — Gravity and magnetic calculations for simple bodies
1943	George P. Woollard — First transcontinental magnetic profile of U. S. A.
1944	Balsley — First aeromagnetic (biplane) survey, Boyertown, Pennsylvania
1945–1955	Graphical depth-to-source techniques are developed
1945	Balsley — First ore deposit discovered from aeromagnetic data, Adirondacks, New York
1946	Balsley — First offshore aeromagnetic survey, coastal Gulf of Mexico
1946	First aeromagnetic maps published
1947	Canada begins systematic national aeromagnetic coverage
1947	First aeromagnetic survey in Australia
1948	First shipborne marine magnetic survey for study of the ocean floor
1949	Convolution methods are developed for derivatives and analytical continuation
1950–1960	Joint aeromagnetic-EM surveys become common for base-metal exploration
	Magnetic basement mapping becomes popular in oil exploration
1951	Vacquier et al. — Interpretation of aeromagnetic maps published by Geological Society of America
1951	Australia begins systematic national aeromagnetic coverage
1951	Finland begins systematic national aeromagnetic coverage
1955	Development of proton precession magnetometer

Date	Event
1955	Werner originates depth-estimation method now known as Werner deconvolution
1957	Baranov — Reduction-to-the-pole and pseudogravity transformation
1958	Dean — Use of Fourier methods for derivatives and analytical continuation
1960	Bott — Iterative inversion of gravity and magnetic data
1962	Development of optically pumped magnetometers
1963	Vine-Matthews-Morley model for seafloor spreading
1964	Cosmos 49 scalar satellite magnetometer is launched
1965–1975	Digital recording of aeromagnetic surveys becomes routine
1965	Talwani — Digital computation of magnetic anomalies
1965	Cooley and Tukey — Development of fast Fourier transform (FFT)
1965	Hood — Gradient measurements for airborne surveying
1965	Hood introduces concept of Euler deconvolution
1967	Fuller — Comprehensive analysis of space-domain filters
1967	First national aeromagnetic map of Canada published
1968	International Geomagnetic Reference Field (IGRF) established
1969	Australia begins collecting joint spectral gamma-ray and aeromagnetic data
1969	Dampney — Equivalent source technique
1970	Spector and Grant — Statistical methods for magnetic interpretation
1971	Naudy — Automatic magnetic depth determination
1971	Hartmann et al. — Implementation of Werner deconvolution
1972	O'Brien — CompuDepth
1972	Nabighian — Analytic Signal
1972	Syberg — Potential field continuation and matched filters
1972	Wiggins — Generalized linear inverse theory
1972	Parker — Fourier modeling of complex topography
1972	Gunn — Wiener filters for transformations of gravity and magnetic fields
1972	Finland completes national high-altitude (150-m) aeromagnetic coverage
1972	Finland begins national low-altitude (40-m) aeromagnetic coverage
1973	Grant — Susceptibility mapping
1973	McGrath and Hood — Multimodel least-squares interpretation
1974–1980	Joint aeromagnetic and gamma-ray surveys of U. S. for uranium exploration
1974	Briggs — Minimum curvature gridding
1975	Zimmerman and Campbell — SQUID magnetometers
1976	First aeromagnetic anomaly map of Australia published
1979	Launch of MAGSAT, the first vector magnetometer satellite mission
1979	First aeromagnetic anomaly map of Soviet Union published
1980	Reid — Aeromagnetic survey design
1980	First aeromagnetic anomaly map of Finland published
1982	Composite magnetic anomaly map of the conterminous U. S. published
1982	Thompson — Euler deconvolution method for 2D depth estimation
1984	Lines and Treitel — Least-squares inversion techniques
1984	Hardwick — Compensation of aircraft magnetic field
1984	Nabighian — 3D Hilbert transforms
1984	Goupillaud et al. — Wavelet transforms for geophysical applications
1980–1990	HRAM surveys flown to test direct detection of hydrocarbons
1985	Cordell and Grauch introduce horizontal gradient method for magnetic data
1985	Cordell introduces chessboard method for continuation to irregular surfaces
1985	Shaded-relief image display of aeromagnetic data becomes popular
1987	Grauch — Magnetic terrain effects
1989	Cordell and McCafferty — Terracing
1990	Reid et al. — 3D Euler deconvolution on gridded data sets
1990–1995	GPS navigation increases location accuracy for airborne surveys
1990–2000	HRAM surveys become standard
1992	Roest et al. — Total gradient
1996	Li and Oldenburg — 3D inversion of magnetic data
1997	Thurston and Smith — SPI (local wavenumber) technique
1997	Moreau et al. — Wavelet analysis of potential fields
1998	Archibald et al. — Multiscale edge analysis of potential field data
1990–2000	GIS and 3D visualization greatly improve magnetic interpretation
2001	Mushayandebvu et al. — Extended Euler deconvolution
2001	Nabighian and Hansen — Unification of Euler and Werner deconvolutions
2002	Hansen — Multisource Werner deconvolution
2002	Hansen and Suciu — Multisource Euler deconvolution
2002	Comprehensive model (CM) proposed as replacement for IGRF
2004	Mushayandebvu et al. — Eigenvalue analysis for the 3D Euler equation

Note: In the space allotted, it is impossible to include all the important stages of development of the magnetic method, and omissions are inevitable.

REFERENCES

Abaco, C. I., and D. C. Lawton, 2003, Magnetic anomalies in the Alberta foothills, Canada: SEG Expanded Abstracts, **22**, 612–615.

Agarwal, R. G., and E. R. Kanasewich, 1971, Automatic trend analysis and interpretation of potential field data: Geophysics, **36**, 339–348.

Agocs, W. B., 1951, Least-squares residual anomaly determination: Geophysics, **16**, 686–696.

Airo, M. -L., 2002, Aeromagnetic and aeroradiometric response to hydrothermal alteration: Surveys in Geophysics, **23**, 273–302.

Allingham, J. W., 1964, Low-amplitude aeromagnetic anomalies in southeastern Missouri: Geophysics, **29**, 537–552.

Andreasen, G. E., and I. Zietz, 1969, Magnetic fields for a 4 × 6 prismatic model: U. S. Geological Survey Professional Paper 666.

Arkani-Hamed, J., 1988, Differential reduction-to-the-pole of regional magnetic anomalies: Geophysics, **53**, 1592–1600.

Ballantyne Jr., E. J., 1980, Magnetic curve fit for a thin dike — Calculator program (TI-59): Geophysics, **45**, 447–455.

Balsley, J. R., 1952, Aeromagnetic surveying, *in* H. E. Landsberg, ed., Advances in Geophysics, 1: Academic Press, 313–350.
Baranov, V., 1957, A new method for interpretation of aeromagnetic maps pseudo-gravimetric anomalies: Geophysics, **22**, 359–383.
Baranov, V., and H. Naudy, 1964, Numerical calculation of the formula of reduction to the magnetic pole: Geophysics, **29**, 67–79.
Barbosa, V. C. F., J. B. C. Silva, and W. E. Medeiros, 1999, Stability analysis and improvement of structural index estimation in Euler deconvolution: Geophysics, **64**, 48–60.
Barnett, C. T., 1976, Theoretical modeling of the magnetic and gravitational fields of an arbitrarily shaped three-dimensional body: Geophysics, **41**, 1353–1364.
Barongo, J. O., 1985, Method for depth estimation and aeromagnetic vertical gradient anomalies: Geophysics, **50**, 963–968.
Bartolino, J. R., and J. C. Cole, 2002, Ground-water resources of the Middle Rio Grande Basin, New Mexico: U. S. Geological Survey Circular 1222.
Barton, C. E., 1997, International Geomagnetic Reference Field: The seventh generation: Journal of Geomagnetism and Geoelectricity, **49**, 123–148.
Batchelor, A., and J. Gutmanis, 2002, Hydrocarbon production from fractured basement reservoirs — version 7: www.geoscience.co.uk/downloads/fracturedbasementver7.pdf.
Bath, G. D., 1968, Aeromagnetic anomalies related to remanent magnetism in volcanic rock, Nevada Test Site: Geological Society of America Memoir 110, 135–146.
Bath, G. D. and C. E. Jahren, 1984, Interpretation of magnetic anomalies at a potential repository site located in the Yucca Mountain area, Nevada Test Site: U. S. Geological Survey Open File Report 84–120.
Bean, R. J., W. F. Fillippone, N. R. Paterson, and I. Zietz, 1961, Discussion of "An evaluation of basement depth determination from airborne magnetometer data," by Peter Jacobsen Jr.: Geophysics, **26**, 317–319.
Bhattacharyya, B. K., 1964, Magnetic anomalies due to prism-shaped bodies with arbitrary polarization: Geophysics, **29**, 517–531.
———, 1965, Two-dimensional harmonic analysis as a tool for magnetic interpretation: Geophysics, **30**, 829–857.
———, 1966, Continuous spectrum of the total-magnetic-field anomaly due to a rectangular prismatic body: Geophysics, **31**, 97–121.
———, 1969, Bicubic spline interpolation as a method for treatment of potential field data: Geophysics, **34**, 402–423.
———, 1980, A generalized multibody model for inversion of magnetic anomalies: Geophysics, **45**, 255–270.
Bhattacharyya, B. K., and K. C. Chan, 1977a, Reduction of magnetic and gravity data on an arbitrary surface acquired in a region of high topographic relief: Geophysics, **42**, 1411–1430.
———, 1977b, Computation of gravity and magnetic anomalies due to inhomogeneous distribution of magnetization and density in a localized region: Geophysics, **42**, 602–609.
Blakely, R. J., 1981, A program for rapidly computing the magnetic anomaly over digital topography: U. S. Geological Survey Open File Report 81–298.
———, 1995, Potential theory in gravity and magnetic applications: Cambridge University Press.
Blakely, R. J., and V. J. S. Grauch, 1983, Magnetic models of crystalline terrane; accounting for the effect of topography: Geophysics, **48**, 1551–1557.
Blakely, R. J., and S. Hassanzadeh, 1981, Estimation of depth to magnetic source using maximum entropy power spectra, with application to the Peru-Chile Trench, Nazca Plate; Crustal formation and Andean convergence: Geological Society of America Memoir 154, 667–682.
Blakely, R. J., and R. W. Simpson, 1986, Approximating edges of source bodies from magnetic or gravity anomalies: Geophysics, **51**, 1494–1498.
Blakely, R. J., V. E. Langenheim, D. A. Ponce, and G. L. Dixon, 2000a, Aeromagnetic survey of the Amargosa Desert, Nevada and California; a tool for understanding near-surface geology and hydrology: U. S. Geological Survey Open File Report 00-0188, http://pubs.usgs.gov/open-file/of00-188/.
Blakely, R. J., R. E. Wells, T. L. Tolan, M. H. Beeson, A. M. Trehu, and L. M. Liberty, 2000b, New aeromagnetic data reveal large strike-slip faults in the northern Willamette Valley, Oregon: Geological Society of America Bulletin, **112**, 1225–1233.
Boardman, J. W., 1985, Magnetic anomalies over oil fields: M.S. thesis, Colorado School of Mines.
Books, K. G., 1962, Remanent magnetism as a contributor to some aeromagnetic anomalies: Geophysics, **27**, 359–375.
Bott, M. H. P., 1960, The use of rapid digital computing methods for direct gravity interpretation of sedimentary basins: Geophysical Journal of the Royal Astronomical Society, **3**, 63–67.
———, 1963, Two methods applicable to computers for evaluating magnetic anomalies due to finite three dimensional bodies: Geophysical Prospecting, **11**, 292–299.
Breiner, S., 1981, Horizontal gradient methods for airborne and marine geophysical exploration: 51st Annual International Meeting, SEG, Expanded Abstracts, Geophysics, 441–442.
Briggs, I. C., 1974, Machine contouring using minimum curvature: Geophysics, **39**, 39–48.
Broding, R. A., C. W. Zimmerman, E. V. Somers, E. S. Wilhelm, and A. A. Stripling, 1952, Magnetic well-logging: Geophysics, **17**, 1–26.
Bush, M. D., R. A. Cayley, S. Rooney, K. Slater, and M. L. Whitehead, 1995, The geology and prospectivity of the southern margin of the Murray Basin: Geological Survey of Victoria VIMP Report 4.
Butler, D. K., 2001, Potential fields methods for location of unexploded ordnance: The Leading Edge, **20**, 890–895.
Byerly, P. E., 1965, Convolution filtering of gravity and magnetic maps: Geophysics, **30**, 281–283.
Cady, J. W., 1980, Calculation of gravity and magnetic anomalies of finite-length right polygonal prisms: Geophysics, **45**, 1507–1512.
Campbell, W. C., 1997, Introduction to geomagnetic fields: Cambridge University Press.
Campos-Enriquez, J. O., R. Diaz-Navarro, J. M. Espindola, and M. Mena, 1996, Chicxulub — Subsurface structure of impact crater inferred from gravity and magnetic data: The Leading Edge, **15**, 357–359.
Chapin, D. A., 1997, Wavelet transforms: A new paradigm for interpreting gravity and magnetics data?: 67th Annual International Meeting, SEG, Expanded Abstracts, 486–489.
Chapin, D. A., S. V. Yalamanchili, and P. H. Daggett, 1998, The St. George Basin, Alaska, COST #1 well: An example of the need for integrated interpretation, *in* R. I. Gibson, and P. S. Millegan, eds., Geologic applications of gravity and magnetics: Case histories: SEG and AAPG.
Clark, D. A., 1983, Comments on magnetic petrophysics: Bulletin of Australian Society of Exploration Geophysicists, **14**, 49–62.
———, 1997, Magnetic petrophysics and magnetic petrology; aids to geological interpretation of magnetic surveys: AGSO Journal of Australian Geology and Geophysics, **17**, 83–103.
Clark, D. A., and D. W. Emerson, 1991, Notes on rock magnetization characteristics in applied geophysical studies: Exploration Geophysics, **22**, 547–555.
Clarke, G. K. C., 1969, Optimum second derivative and downward continuation filters: Geophysics, **34**, 424–437.
Committee for the Magnetic Anomaly Map of North America, 1987, Magnetic anomaly map of North America: Geological Society of America Continent Scale Map 003.
Cook, D. G., and B. C. MacLean, 1999: The Imperial Anticline, a fault-bend fold above a bedding-parallel thrust ramp, Northwest Territories, Canada: Journal of Structural Geology, **21**, 215–228.
———, 2004: Subsurface Proterozoic stratigraphy and tectonics of the western plains of the Northwest Territories. Geological Survey of Canada, Bulletin 575.
Cooper, G. R. J., and D. R. Cowan, 2003, Sunshading geophysical data using fractional order horizontal gradients: The Leading Edge, **22**, 204.
Cordell, L., 1979, Gravimetric expression of graben faulting in Santa Fe County and the Espanola Basin, New Mexico, *in* R. V. Ingersoll, ed., Guidebook to Santa Fe County: 30th Field Conference, New Mexico Geological Society, 59–64.
———, 1985a, Applications and problems of analytical continuation of New Mexico aeromagnetic data between arbitrary surfaces of very high relief: Proceedings of International Meeting on Potential Fields in Rugged Topography, Institut de Géophysique de Université de Lausanne, Bulletin 7, 96–101
———, 1985b, A stripping filter for potential field data: SEG, Expanded Abstracts, 55th Annual International Meeting, SEG, Expanded Abstracts, 217–218.
———, 1992, A scattered equivalent-source method for the interpolation and gridding of potential-field data in three dimensions: Geophysics, **57**, 629–636.
Cordell, L., and V. J. S. Grauch, 1982, Mapping basement magnetization zones from aeromagnetic data in the San Juan Basin, New Mexico: 52nd Annual International Meeting, SEG, Expanded Abstracts, 246–247.
———, 1985, Mapping basement magnetization zones from aeromagnetic data in the San Juan Basin New Mexico, *in* W. J. Hinze, ed., Utility of regional gravity and magnetic maps: SEG, 181–197.
Cordell, L., and D. H. Knepper, 1987, Aeromagnetic images: Fresh in-

sight to the buried basement, Rolla quadrangle, southeast Missouri: Geophysics, **52**, 218–231.
Cordell, L., and A. E. McCafferty, 1989, A terracing operator for physical property mapping with potential field data: Geophysics, **54**, 621–634.
Cowan, D. R., and S. Cowan, 1993, Separation filtering applied to aeromagnetic data: Exploration Geophysics, **24**, 429–436.
Cox, A., 1973, Plate tectonics and geomagnetic reversals: W. H. Freeman and Company.
Craig, M., 1996, Analytic signals for multivariate data: Mathematical Geology, **28**, 315–329.
Cribb, J., 1976, Application of the generalized linear inverse to the inversion of static potential data: Geophysics, **41**, 1365–1369.
Davies, J., M. F. Mushayandebvu, and R. Smith, 2004, Magnetic detection and characterization of Tertiary and Quaternary buried channels: 74th Annual International Meeting, SEG, Expanded Abstracts, 734.
Dean, W. C., 1958, Frequency analysis for gravity and magnetic interpretation: Geophysics, **23**, 97–127.
Dickinson, M., 1986, A search for intra-sedimentary aeromagnetic anomalies over a known oil field in the Denver Basin: M.S. thesis, Colorado School of Mines.
Dietz, R. S., 1961, Continent and ocean basin evolution by spreading of the sea floor: Nature, **190**, 854–857.
Eaton, D., and K. Vasudevan, 2004, Skeletonization of aeromagnetic data: Geophysics, **69**, 478–488.
EG&G Geometrics (ca.1970s), A guide to passive magnetic compensation of aircrafts: EG&G Geometrics Technical Report Number 15.
Fairhead, J. D., J. D. Misener, C. M. Green, G. Bainbridge, and S. W. Reford, 1997, Large scale compilations of magnetic, gravity, radiometric and electromagnetic data: The new exploration strategy for the 90s, *in* A. G. Gubins, ed., Proceedings of Exploration 97: Fourth Decennial International Conference on Mineral Exploration, 805–816.
Finn, C. A., ed., 2002, Examples of the utility of magnetic anomaly data for geologic mapping: U. S. Geological Survey Open-file Report 02-0400, available at http://pubs.usgs.gov/of/2002/ofr-02-0400/
Finn, C. A., T. W. Sisson, and M. Deszcz-Pan, 2001, Aerogeophysical measurements of collapse-prone hydrothermally altered zones at Mount Rainier Volcano: Nature, **409**, 600–603.
Finn, C. A., and L. A. Morgan, 2002, High-resolution aeromagnetic mapping of volcanic terrain, Yellowstone National Park: Journal of Volcanology and Geothermal Research, **115**, 207–231.
Fitzgerald, D., A. Reid, and P. McInerney, 2003, New discrimination techniques for Euler deconvolution: 8th South African Geophysical Association (SAGA) Biennial Technical Meeting and Exhibition.
Frischknecht, F. C., L. Muth, R. Grette, T. Buckley, and B. Kornegay, 1983, Geophysical methods for locating abandoned wells: U. S. Geological Survey Open File Report 83–702.
Frowe, E., 1948, A total field magnetometer for mobile operation: Geophysics, **13**, 209–214.
Fuller, B. D., 1967, Two-dimensional frequency analysis and design of grid operators, *in* Mining Geophysics, II: Society of Exploration Geophysicists, 658–708.
Gay Jr., S. P., 1992, Epigenetic versus syngenetic magnetite as a cause of magnetic anomalies: Geophysics, **57**, 60–68.
———, 2004, Glacial till: A troublesome source of near-surface magnetic anomalies: The Leading Edge, **23**, 542–547.
Gay, S. P., and B. W. Hawley, 1991, Syngenetic magnetic anomaly sources: Three examples: Geophysics, **56**, 902–913.
Geological Survey of Canada, 2005, Canadian Aeromagnetic Data Base, Central Canada Division, Earth Sciences Sector, Natural Resources Canada.
Gerovska, D., and M. J. Araúzo-Bravo, 2003, Automatic interpretation of magnetic data based on Euler deconvolution with unprescribed structural index: Computers & Geosciences, **29**, 949–960.
Gibson, R. I., and P. S. Millegan, eds., 1998, Geologic applications of gravity and magnetics: Case histories: SEG and AAPG.
Goldhaber, M. B., and R. L. Reynolds, 1991, Relations among hydrocarbon reservoirs, epigenetic sulfidization, and rock magnetization: Examples from the south Texas coastal plain: Geophysics, **56**, 748–757.
Goupillaud, P. L., A. Grossmann, and J. Morlet, 1984, Cycle-octave and related transforms in seismic signal analysis: Geoexploration, **23**, 85–102.
Goussev, S. A., R. A. Charters, J. W. Peirce, and W. E. Glenn, 2003, Jackpine magnetic anomaly: Identification of a buried meteorite impact structure: The Leading Edge, **22**, 740–741.
Goussev, S. A., L. Griffith, J. Peirce, and A. Cordsen, 2004, Enhanced HRAM anomalies correlate faults between 2D seismic lines: 74th Annual International Meeting, SEG, Extended Abstracts, 730.
Grant, F. S., 1972, Review of data processing and interpretation methods in gravity and magnetics, 1964–71: Geophysics, **37**, 647–661.
Grant, F. S., 1973, The magnetic susceptibility mapping method for interpreting aeromagnetic surveys: 43rd Annual International Meeting, SEG, Expanded Abstracts, 1201.
———, 1985, Aeromagnetics, geology and ore environments, *in* Magnetite in igneous, sedimentary and metamorphic rocks: An overview: Geoexploration, **23**, 303–333.
Grant, F. S., and L. Martin, 1966, Interpretation of aeromagnetic anomalies by the use of characteristic curves: Geophysics, **31**, 135–148.
Grauch, V. J. S., 1987, A new variable-magnetization terrain correction method for aeromagnetic data: Geophysics, **52**, 94–107.
Grauch, V. J. S., and L. Cordell, 1987, Limitations on determining density or magnetic boundaries from the horizontal gradient of gravity or pseudogravity data: Geophysics, **52**, 118–121.
Grauch, V. J. S., and C. S. Johnston, 2002, Gradient window method: A simple way to separate regional from local horizontal gradients in gridded potential-field data: 72nd Annual International Meeting, SEG, Expanded Abstracts, 762–765.
Grauch, V. J. S., D. A. Sawyer, C. J. Fridrich, and M. R. Hudson, 1999, Geophysical framework of the southwestern Nevada volcanic field and hydrogeologic implications: U. S. Geological Survey Professional Paper1608.
Grauch, V. J. S., M. R. Hudson, and S. A. Minor, 2001, Aeromagnetic expression of faults that offset basin fill, Albuquerque basin, New Mexico: Geophysics, **66**, 707–720.
Griffin, W. R., 1949, Residual gravity in theory and practice: Geophysics, **14**, 39–56.
Grivet, P. A., and L. Malnar, 1967, Measurement of weak magnetic fields by magnetic resonance: Advances in Electronics and Electron Physics, **23**, 39–151.
Guillen, A., and V. Menichetti, 1984, Gravity and magnetic inversion with minimization of a specific functional: Geophysics, **49**, 1354–1360.
Gunn, P. J., 1972, Application of Wiener filters to transformations of gravity and magnetic fields: Geophysical Prospecting, **20**, 860–871.
———, 1975, Linear transformations of gravity and magnetic fields: Geophysical Prospecting, **23**, 300–312.
———, 1995, An algorithm for reduction to the pole that works at all magnetic latitudes: Exploration Geophysics, **26**, 247–254.
———, 1997, Application of aeromagnetic surveys to sedimentary basin studies: AGSO Journal of Australian Geology and Geophysics, **17**, 133–144.
———, 1998, Aeromagnetics locates prospective areas and prospects: The Leading Edge, **17**, 67–69.
Gunn, P. J., D. FitzGerald, and N. Yassi, 1996, Complex attributes: New tools for enhancing aeromagnetic data: Australian Geological Survey Organization (AGSO) Research Newsletter, no. 25, 16–17.
Guspi, F., and B. Introcaso, 2000, A sparse spectrum technique for gridding and separating potential field anomalies: Geophysics, **65**, 1154–1161.
Haggerty, S. E., 1979, The aeromagnetic mineralogy of igneous rocks: Canadian Journal of Earth Sciences, **16**, 1281–1293.
Hall, S. H., 1962, The modulation of a proton magnetometer signal due to rotation: Geophysical Journal, **7**, 131–142.
Hammer, S., 1963, Deep gravity interpretation by stripping: Geophysics, **28**, 369–378.
Haney, M., and Y. Li, 2002, Total magnetization direction and dip from multiscale edge: 72nd Annual International Meeting, SEG, Expanded Abstracts, 735–738.
Haney, M., C. Johnston, Y. Li, and M. Nabighian, 2003, Envelopes of 2D and 3D magnetic data and their relationship to the analytic signal: Preliminary results: 73rd Annual International Meeting, SEG Expanded Abstracts, 596–599.
Hanna, W. F., 1990, Some historical notes on early magnetic surveying in the U. S. Geological Survey, *in* W. F. Hanna, ed., Geologic applications of modern aeromagnetic surveys: U. S. Geological Survey Bulletin 1924, 63–73.
Hansen, R. O., 1984, Two approaches to total field reconstruction from gradiometer data: 54th Annual International Meeting, SEG Expanded Abstracts, 245.
———, 1993, Interpretative gridding by anisotropic kriging: Geophysics, **58**, 1491–1497.
———, 2002, 3D multiple-source Werner deconvolution: 72nd Annual International Meeting, SEG, Expanded Abstracts, 802–805.
Hansen, R. O., and Y. Miyazaki, 1984, Continuation of potential fields between arbitrary surfaces: Geophysics, **49**, 787–795.
Hansen, R. O., and R. S. Pawlowski, 1989, Reduction-to-the-pole at low latitudes by Wiener filtering: Geophysics, **54**, 1607–1613.

Hansen, R. O., and M. Simmonds, 1993, Multiple-source Werner deconvolution: Geophysics, **58**, 1792–1800.
Hansen, R. O., and L. Suciu, 2002, Multiple-source Euler deconvolution: Geophysics, **67**, 525–535.
Hardwick, C. D., 1984, Important design considerations for inboard airborne magnetic gradiometers: Geophysics, **49**, 2004–2018.
Hartman, R. R., D. J. Teskey, and J. L. Friedberg, 1971, A system for rapid digital aeromagnetic interpretation: Geophysics, **36**, 891–918.
Hassan, H. H., and J. W. Peirce, 2005, SAUCE: A new technique to remove cultural noise from HRAM: The Leading Edge, **24**, 246–250.
Hassan, H. H., J. W. Peirce, W. C. Pearson, and M. J. Pearson, 1998, Cultural editing of HRAM data: Comparison of techniques: Canadian Journal of Exploration Geophysics, **34**, www.cseg.ca.
Heezen, B. C., M. Ewing, and E. T. Miller, 1953, Trans-Atlantic profile of total magnetic intensity and topography: Dakar to Barbados: Deep Sea Research, **1**, 25–23.
Heiland, C. A., 1935, Geophysical mapping from the air: Its possibilities and advantages: Engineering and Mining Journal, **136**, 609–610.
———, 1940, Geophysical Exploration: Prentice Hall.
Heiland, C. A., and W. H. Courtier, 1929, Magnetometric investigation and gold placer deposits near Golden (Jefferson County), Colorado: Transactions of the American Institute of Mining, Metallurgical and Petroleum Engineers (AIME), **81**, 364–384.
Henderson, R., 1960, A comprehensive system of automatic computation in magnetic and gravity interpretation: Geophysics, **25**, 569–585.
Henderson, R. G., and I. Zietz, 1948, Analysis of total magnetic intensity anomalies produced by point and line sources: Geophysics, **13**, 428–436.
———, 1949, The computation of second vertical derivatives of geomagnetic fields: Geophysics, **14**, 508–516.
Hess, H. H., 1962, History of ocean basins, *in* A. E. J. Engel, H. L. James, and B. F. Leonard, eds., Petrologic studies: A volume to honor A. F. Buddington: Geological Society of America, 599–620.
Hildenbrand, T. G., and G. . Raines, 1990, Need for aeromagnetic data and a national airborne geophysics program: U. S. Geological Survey Bulletin 1924, 1–5.
Hinze, W. J., 1985a, ed., Proceedings of the International Meeting on Potential Fields in Rugged Topography: Institut de Géophysique de Université de Lausanne, Bulletin no. 7.
———, 1985b, ed., The utility of regional gravity and magnetic anomaly maps: SEG, 181–197.
Hjelt, S. E., 1972, Magnetostatic anomalies of a dipping prism: Geoexploration, **10**, 239–254.
Hogg, R. L. S., 1979, Illustration of a new Northway process for eliminating the "herringbone" component from problem geophysical data: Annual Meeting of Canadian Society of Exploration Geophysicists.
Holstein, H., 2002a, Gravimagnetic similarity in anomaly formulas for uniform polyhedra: Geophysics, **67**, 1126–1133.
Holstein, H., 2002b, Invariance in gravimagnetic anomaly formulas for uniform polyhedra: Geophysics, **67**, 1134–1137.
Hood, P. J., 1990, Aeromagnetic survey program of Canada, mineral applications, and vertical gradiometry, *in* W. F. Hanna, ed., Geologic applications of modern aeromagnetic surveys: U. S. Geological Survey Bulletin 1924, 7–23.
Hornby, P., F. Boschetti, and F. G. Horowitz, 1999, Analysis of potential field data in the wavelet domain: Geophysical Journal International, **137**, 175–196.
Hoylman, H. W., 1961, How to determine and remove diurnal effects precisely: World Oil, December, 107–112.
Huang, D., and P. A. Versnel, 2000, Depth estimation algorithm applied to FTG data: 70th Annual International Meeting, SEG, Expanded Abstracts, 394–397.
Hutchison, R. D., 1958, Magnetic analysis by logarithmic curves: Geophysics, **23**, 749–769.
Jacobsen, B., 1987, A case for upward continuation as a standard separation filter for potential-field maps: Geophysics, **52**, 1138–1148.
Jacobson Jr., P., 1961, An evaluation of basement depth determinations from airborne magnetometer data: Geophysics, **26**, 309–317.
Jain, S., 1976, An automatic method of direct interpretation of magnetic profiles: Geophysics, **41**, 531–545.
Jakosky, J. J., 1950, Exploration geophysics: Trija Publishing Company.
Jenny, W. P., 1936, Micromagnetic surveys: Gulf Coast structures may be outlined by this new method: The Oil Weekly, April 27.
Jensen, H., 1965, Instrument details and application of a new airborne magnetometer: Geophysics, **30**, 875–882.
Jessell, M. W., 2001, Three-dimensional modeling of potential-field data: Computers & Geosciences, **27**, 455–465.
Jessell, M. W., and Fractal Geophysics Pty Ltd., 2002, An atlas of structural geophysics II: Journal of the Virtual Explorer, **5**, http://www.mssu.edu/seg-vm/exhibits/structuraatlas/index.html.
Jessell, M. W., and R. K. Valenta, 1996, Structural geophysics: Integrated structural and geophysical mapping, *in* D. DePaor, ed., Structural geology and personal computers: Elsevier Science Publishing Co., 303–324.
Jessell, M. W., R. K. Valenta, G. Jung, J. P. Cull, and A. Gerio, 1993, Structural geophysics: Exploration Geophysics, **24**, 599–602.
Johnson, R. C., T.M. Finn, and V. F. Nuccio, 2001, Potential for a basin-centered gas accumulation in the Albuquerque Basin, New Mexico: U. S. Geological Survey Bulletin 2184-C, available online at http://pubs.usgs.gov/bul/b2184-c/.
Josephson, B. D., 1962, Possible new effect in superconductive tunneling: Physics Letters, **1**, 251–253.
Keating, P., 1993, The fractal dimension of gravity data sets and its implication for gridding: Geophysical Prospecting, **41**, 983–994.
———, 1995, A simple technique to identify magnetic anomalies due to kimberlite pipes: Exploration Mining Geology, **4**, 121–125.
Keating, P., and M. Pilkington, 2000, Euler deconvolution of the analytic signal: 62nd Annual International Meeting, EAGE, Session P0193.
Keating, P., and L. Zerbo, 1996, An improved technique for reduction to the pole at low latitudes: Geophysics, **61**, 131–137.
Kellogg, O. D., 1953, Foundations of potential theory: Dover Publications.
Kilty, K. T., 1983, Werner deconvolution of profile potential field data: Geophysics, **48**, 234–237.
Korhonen, J. V., H. Säävuori, and T. Koistinen, 2003, Petrophysical correlation of Fennoscandian magnetic and gravity anomalies: European Geophysical Society (EGS) –American Geophysical Union (AGU)–European Union of Geosciences (EUG) Joint Assembly, abstract #13230.
Koulomzine, T., Y. Lamontagne, and A. Nadeau, 1970, New methods for the direct interpretation of magnetic anomalies caused by inclined dikes of infinite length: Geophysics, **35**, 812–830.
Ku, C. C., and J. A. Sharp, 1983, Werner deconvolution for automated magnetic interpretation and its refinement using Marquardt inverse modeling: Geophysics, **48**, 754–774.
Langel, R. A., 1992, International Geomagnetic Reference Field: The sixth generation: Journal of Geomagnetism and Geoelectricity, **44**, 679–707.
Langel, R. A., and W. J. Hinze, 1998, The magnetic field of the Earth's lithosphere: The satellite perspective: Cambridge University Press.
Langenheim, V. E., R. C. Jachens, D. M. Morton, R. W. Kistler, and J. C. Matti, 2004, Geophysical and isotopic mapping of preexisting crustal structures that influenced the location and development of the San Jacinto fault zone, southern California: Geological Society of America Bulletin, **116**, 1143–1157.
Leblanc, G., and W. A. Morris, 2001, Denoising of aeromagnetic data via the wavelet transform: Geophysics, **66**, 1793–1804.
Leliak, P., 1961, Identification and evaluation of magnetic-field sources of magnetic airborne detector equipped aircraft: IRE Transactions on Aerospace and Navigational Electronics, **8**, 95–106.
Leu, L., 1982, Use of reduction-to-the-equator process for magnetic data interpretation: Geophysics, **47**, 445
Levanto, A. E., 1959, A three-component magnetometer for small drill holes and its use in ore prospecting: Geophysical Prospecting, **7**, 183–195
Li, Y., and D. W. Oldenburg, 1996, 3-D inversion of magnetic data: Geophysics, **61**, 394–408.
———, 1998a, Separation of regional and residual magnetic field data: Geophysics, **63**, 431–439.
———, 1998b, Stable reduction to the pole at the magnetic equator: 68th Annual International Meeting, SEG, Expanded Abstracts, 533–536.
———, 1999, Rapid construction of equivalent sources using wavelets: 60th Annual International Meeting, SEG, Expanded Abstracts, 374–377.
———, 2000a, Reduction to the pole using equivalent sources: 60th Annual International Meeting, SEG, Expanded Abstracts, 386–389.
———, 2000b, Joint inversion of surface and three-component borehole magnetic data: Geophysics, **65**, 540–552.
———, 2003, Fast inversion of large-scale magnetic data using wavelet transforms and logarithmic barrier method: Geophysical Journal International, **152**, 251–265.
Logachev, A. A., 1946, The development and application of airborne magnetometers in the U.S.S.R.: Geophysics, **11**, 135–147.
Lundberg, H., 1947, Results obtained by a helicopter borne magnetometer: Transactions, Canadian Institute of Mining and Metallurgy, **50**, 392–400.

Macdonald, K. C., S. P. Miller, S. P. Huestis, and F. N. Spiess, 1980, Three-dimensional modeling of a magnetic reversal boundary from inversion of deep-tow measurements: Journal of Geophysical Research, **85**, 3670–3680.
Machel, H. G., and E. A. Burton, 1991, Chemical and microbial processes causing anomalous magnetization in environments affected by hydrocarbon seepage: Geophysics, **56**, 598–605.
MacLean, B. C., and D. G. Cook, 2002(updated), Subsurface and surface distribution of Proterozoic units, northwestern NWT: a Cambrian sub-crop map: Geological Survey of Canada, Open File 3502.
Macmillan, S., S. Maus, T. Bondar, A. Chambodut, V. Golovkov, R. Holme, B. Langlais et al., 2003, Ninth generation International Geomagnetic Reference Field released: EOS Transactions of the American Geophysical Union, **84**, 503.
Macnae, J. C., 1979, Kimberlites and exploration geophysics: Geophysics, **44**, 1395–1416.
Mason, R. G., 1958, A magnetic survey off the west coast of the United States between latitudes 30° and 36° N, longitudes 121° and 128° W: Geophysical Journal of the Royal Astronomical Society, **1**, 320–329.
Maus, S., 1999, Variogram analysis of magnetic and gravity data: Geophysics, **64**, 776–784.
Maus, S., K. P. Sengpiel, B. Rottger, and E. A. W. Tordiffe, 1999, Variogram analysis of helicopter magnetic data to identify paleochannels of the Omaruru River, Namibia: Geophysics, **64**, 785–794.
Maus, S., and S. Macmillan, 2005, 10th generation International Geomagnetic Reference Field: EOS Transactions of the American Geophysical Union, **86**, 159.
Maxwell, A. E., R. P. von Herzen, et al., 1970, Initial Reports of the Deep Sea Drilling Project; covering Leg 3 of the cruises of the drilling vessel "Glomar Challenger," Dakar, Senegal to Rio de Janeiro, Brazil, December 1968 to January 1969: Deep Sea Drilling Project: U. S. Government Printing Office.
Mazur, M. J., R. R. Stewart, and A. R. Hildebrand, 2000, The seismic signature of meteorite impact craters: Canadian Society of Exploration Geophysicists Recorder, **35**, June, 10–16.
McConnell, T. J., B. Lo, A. Ryder-Turner, and J. A. Musser, 1999, Enhanced 3D seismic surveys using a new airborne pipeline mapping system: 69th Annual International Meeting, SEG, Expanded Abstracts, 516–519.
McElhinny, M. W., 1973, Paleomagnetics and plate tectonics: Cambridge University Press.
McIntyre, J. I., 1980, Geological significance of magnetic patterns related to magnetite in sediments and metasediments — A review: Bulletin of the Australian Society of Exploration Geophysicists, **11**, 19–33.
Mendonça, C. A., and J. B. C. Silva, 1993, A stable truncated series approximation of the reduction-to-the-pole operator: Geophysics, **58**, 1084–1090.
———, 1994, The equivalent data concept applied to the interpolation of potential-field data: Geophysics, **59**, 722–732.
———, 1995, Interpolation of potential-field data by equivalent layer and minimum curvature: A comparative analysis: Geophysics, **60**, 399–407.
Mesko, A., 1965, Some notes concerning the frequency analysis for gravity interpretation: Geophysical Prospecting, **13**, 475–488.
Millegan, P. S., 1998, High-resolution aeromagnetic surveying, *in* R. I. Gibson, and P. S. Millegan, eds., Geologic applications of gravity and magnetics: Case histories: SEG and AAPG.
Miller, H. G., and V. Singh, 1994, Potential field tilt; a new concept for location of potential field sources: Journal of Applied Geophysics, **32**, 213–217.
Minty, B. R. S., 1991, Simple microlevelling for aeromagnetic data: Exploration Geophysics, **22**, 591–592.
Misener, D. J., F. S. Grant, and P. Walker, 1984, Variable depth, space-domain magnetic susceptibility mapping: 54th Annual International Meeting, SEG, Expanded Abstracts, 237.
Mittal, P. K., 1984, Algorithm for error adjustment of potential-field data along a survey network: Geophysics, **49**, 467–469.
Modisi, M. P., E. A. Atekwana, A. B. Kampunzu, and T. H. Ngwisanyi, 2000, Rift kinematics during the incipient stages of continental extension: Evidence from the nascent Okavango rift basin, northwest Botswana: Geology, **28**, 939–942.
Moore, D. H., 2005, Swan Hill 1:250,000 and parts of Balranald and Deniliquin 1:250,000 map areas: A geological interpretation of the geophysical data: Victorian Initiative for Minerals and Petroleum Report 84, Department of Primary Industries, Victoria, Australia.
Moreau, F., D. Gibert, M. Holschneider, and G. Saracco, 1997, Wavelet analysis of potential fields: Inverse Problems, **13**, 165–178.
Morgan, R., 1998, Magnetic anomalies associated with the North and South Morecambe Fields, U. K., *in* R. I. Gibson, and P. R. Milligan, eds., Geologic applications of gravity and magnetics: Case histories: SEG and AAPG, 89–91.
Morley, L. W., 1963, The geophysics division of the Geological Survey of Canada: Bulletin of the Canadian Institute of Mining Metallurgy, **5**, 358–364.
———, 2001, The zebra pattern, *in* N. Orestes, ed., Plate tectonics: An insider's history of the modern theory of the Earth: Westview Press, 67–85.
Morley, L. W., and A. Larochelle, 1964, Paleomagnetism as a means of dating geological events: Royal Society of Canada Special Publication 8, 39–50.
Mushayandebvu, M., A. Reid, and D. Fairhead, 2000, Grid Euler deconvolution with constraints for 2-D structures: 70th Annual International Meeting, SEG, Expanded Abstracts, 398–401.
Mushayandebvu, M. F., P. van Driel, A. B. Reid, and J. D. Fairhead, 2001, Magnetic source parameters of two-dimensional structures using extended Euler deconvolution: Geophysics, **66**, 814–823.
Mushayandebvu, M. F., V. Lesur, A. B. Reid, and J. D. Fairhead, 2004, Grid Euler deconvolution with constraints for 2D structures: Geophysics, **69**, 489–496.
Nabighian, M. N., 1972, The analytic signal of two-dimensional magnetic bodies with polygonal cross-section — Its properties and use for automated anomaly interpretation: Geophysics, **37**, 507–517.
———, 1974, Additional comments on the analytic signal of two-dimensional magnetic bodies with polygonal cross-section: Geophysics, **39**, 85–92.
———, 1984, Toward a three-dimensional automatic interpretation of potential field data via generalized Hilbert transforms — Fundamental relations: Geophysics, **49**, 780–786.
Nabighian, M. N., and R. O. Hansen, 2001, Unification of Euler and Werner deconvolution in three dimensions via the generalized Hilbert transform: Geophysics, **66**, 1805–1810.
Naudy, H., 1971, Automatic determination of depth on aeromagnetic profiles: Geophysics, **36**, 717–722.
Naudy, H., and H. Dreyer, 1968, Essai de filtrage non-lineaire appliqué aux profiles aeromagnetiques (Attempt to apply nonlinear filtering to aeromagnetic profiles): Geophysical Prospecting, **16**, 171–178.
Nettleton, L. L., 1942, Gravity and magnetic calculations: Geophysics, **7**, 293–310.
———, 1971, Elementary gravity and magnetics for geologists and seismologists: SEG.
North American Magnetic Anomaly Group, 2002, Magnetic anomaly map of North America: U. S. Geological Survey Special Map, available online at http://pubs.usgs.gov/sm/mag_map/.
O'Brien, D. P., 1972, CompuDepth, a new method for depth-to-basement computation: Presented at the 42nd Annual International Meeting, SEG.
O'Connell, M. D., 2001, A heuristic method of removing micropulsations from airborne magnetic data: The Leading Edge, **20**, 1242–1244.
O'Connell, M. D., R. S. Smith, and M. A. Vallée, 2005, Gridding aeromagnetic data using longitudinal and transverse gradients with the minimum curvature operator: The Leading Edge, **24**, 142–145.
Okabe, M., 1979, Analytical expressions for gravity anomalies due to homogeneous polyhedral bodies and translations into magnetic anomalies: Geophysics, **44**, 730–741.
Oldenburg, D. W., Y. Li, C. G. Farquharson, P. Kowalczyk, T. Aravanis, A. King, P. Zhang, and A. Watts, 1998, Applications of geophysical inversions in mineral exploration: The Leading Edge, **17**, 461–465.
Olsen, N., R. Holm, G. Hulot, T. Sabaka, T. Neubert, L. Tøffner-Clausen, F. Primdahl, et al., 2000, Ørsted initial field model: Geophysical Research Letters, **27**, 3607.
Oreskes, N., 2001, Plate tectonics: An insider's history of the modern theory of the Earth: Westview Press.
Parker, R. L., 1972, The rapid calculation of potential anomalies: Geophysical Journal of the Royal Astronomical Society, **31**, 447–455.
Parker, R. L., and S. P. Huestis, 1974, Inversion of magnetic anomalies in the presence of topography: Journal of Geophysical Research, **79**, 1587–1593.
Parker, R. L., and K. D. Klitgord, 1972, Magnetic upward continuation from an uneven track: Geophysics, **37**, 662–668.
Paterson, N. R., and C. V. Reeves, 1985, Applications of gravity and magnetic surveys — The state of the art in 1985: Geophysics, **50**, 2558–2594.
Pawlowski, R. S., and R. O. Hansen, 1990, Gravity anomaly separation by Wiener filtering: Geophysics, **55**, 539–548.
Pearson, W. C., 1996, Removing culture from southern Texas — A magnetic clean-up and imaging revolution: 66th Annual International Meeting, SEG, Expanded Abstracts, 1407–1410.
———, 2001, Finding faults in a gas play: AAPG Explorer, May, 52–55.

Pearson, W. C., and C. M. Skinner, 1982, Reduction-to-the-pole of low latitude magnetic anomalies: 52nd Annual International Meeting, SEG, Expanded Abstracts, 356.
Peddie, N. W., 1982, International Geomagnetic Reference Field: The third generation: Journal of Geomagnetism and Geoelectricity, **34**, 309–326.
———, 1983, International Geomagnetic Reference Field — Its evolution and the difference in total field intensity between new and old models for 1965–1980: Geophysics, **48**, 1691–1696.
Pedersen, L. B., 1977, Interpretation of potential field data — A generalized inverse approach: Geophysical Prospecting, **25**, 199–230.
———, 1978, Wavenumber domain expressions for potential fields from arbitrary 2-, $2\frac{1}{2}$-, and 3-dimensional bodies: Geophysics, **43**, 626–630.
———, 1979, Constrained inversion of potential field data: Geophysical Prospecting, **27**, 726–748.
Peirce, J. W., W. E. Glenn, and K. Brown, eds., 1998, High resolution aeromagnetics for hydrocarbon exploration: Canadian Journal of Exploration Geophysics, **34**, available online at www.cseg.ca.
Peirce, J. W., S. A. Goussev, R. McLean, and M. Marshall, 1999, Aeromagnetic interpretation of the Dianango Trough HRAM survey, onshore Gabon: 69th Annual International Meeting, SEG, Extended Abstracts, 343–346.
Peters, L. J., 1949, The direct approach to magnetic interpretation and its practical application: Geophysics, **14**, 290–320.
Phillips, J. D., 1979, ADEPT, A program to estimate depth to magnetic basement from sampled magnetic profiles: U. S. Geological Survey Open File Report No. 79-367.
———, 2000, Locating magnetic contacts: A comparison of the horizontal gradient, analytic signal, and local wavenumber methods: 70th Annual International Meeting, SEG, Expanded Abstracts, 402–405.
———, 2001, Designing matched bandpass and azimuthal filters for the separation of potential-field anomalies by source region and source type: 15th Geophysical Conference and Exhibition, Australian Society of Exploration Geophysicists, Expanded Abstracts, CD-ROM.
———, 2002, Two-step processing for 3D magnetic source locations and structural indices using extended Euler or analytic signal methods: 72nd Annual International Meeting, SEG, Expanded Abstracts, 727–730.
Phillips, J. D., R. W. Saltus, and R. L. Reynolds, 1998, Sources of magnetic anomalies over a sedimentary basin: Preliminary results from the Coastal Plain of the Arctic National Wildlife Refuge, Alaska, *in* R. I. Gibson and P. S. Millegan, eds., Geologic applications of gravity and magnetics: Case histories: SEG and AAPG, 130–134.
Pilkington, M., 1997, 3-D magnetic imaging using conjugate gradients: Geophysics, **62**, 1132–1142.
Pilkington, M., and D. J. Crossley, 1986, Determination of crustal interface topography from potential fields: Geophysics, **51**, 1277–1284.
Pilkington, M., and P. Keating, 2004, Contact mapping from gridded magnetic data — A comparison of techniques: Exploration Geophysics, **35**, 306–311.
Pilkington, M., M. E. Gregotski, and J. P. Todoeschuck, 1994, Using fractal crustal magnetization models in magnetic interpretation: Geophysical Prospecting, **42**, 677–692.
Plouff, D., 1975, Derivation of formulas and FORTRAN programs to compute magnetic anomalies of prisms: National Technical Information Service No. PB-243-525, U. S. Department of Commerce.
———, 1976, Gravity and magnetic fields of polygonal prisms and application to magnetic terrain corrections: Geophysics, **41**, 727–741.
Power, M., G. Belcourt, and E. Rockel, 2004, Geophysical methods for kimberlite exploration in northern Canada: The Leading Edge, **23**, 1124
Prieto, C., and G. Morton, 2003, New insights from a 3D earth model, deepwater Gulf of Mexico: The Leading Edge, **22**, 356–360.
Pustisek, A. M., 1990, Noniterative three-dimensional inversion of magnetic data: Geophysics, **55**, 782–785.
Rasmussen, R., and L. B. Pedersen, 1979, End corrections in potential field modeling: Geophysical Prospecting, **27**, 749–760.
Ravat, D., T. G. Hildenbrand, and W. Roest, 2003, New way of processing near-surface magnetic data: The utility of the Comprehensive Model of the magnetic field: The Leading Edge, **22**, 784–785.
Reford, M. S., 1980, History of geophysical exploration — Magnetic method: Geophysics, **45**, 1640–1658.
Reford, M. S., and J. S. Sumner, 1964, Aeromagnetics: Geophysics, **29**, 482–516.
Reid, A. B., 1980, Aeromagnetic survey design: Geophysics, **45**, 973–976.
Reid, A. B., J. M. Allsop, H. Granser, A. J. Millett, and I. W. Somerton, 1990, Magnetic interpretation in three dimensions using Euler deconvolution: Geophysics, **55**, 80–91.
Reigber, C., H. Luehr, and P. Schwintzer, 2002, CHAMP mission status: Advances in Space Research, **30**, 289–293.
Reynolds, R. L., J. G. Rosenbaum, M. R. Hudson, and N. S. Fishman, 1990, Rock magnetism, the distribution of magnetic minerals in the Earth's crust, and aeromagnetic anomalies: U. S. Geological Survey Bulletin1924, 24–45.
Reynolds, R. L., M. Webring, V. J. S. Grauch, and M. Tuttle, 1990, Magnetic forward models of Cement oil field, Oklahoma, based on rock magnetic, geochemical and petrologic constraints: Geophysics, **55**, 344–353.
Reynolds, R. L., N. S. Fishman, and M. R. Hudson, 1991, Sources of aeromagnetic anomalies over Cement oil field (Oklahoma), Simpson oil field (Alaska), and the Wyoming-Idaho-Utah thrust belt: Geophysics, **56**, 606–617.
Rhodes, J., and J. W. Peirce, 1999, MaFIC — Magnetic interpretation in 3-D using a seismic workstation: 69th Annual International Meeting, SEG, Expanded Abstracts, 335–338.
Ridsdill-Smith, T. A., 1998a, Separating aeromagnetic anomalies using wavelet matched filters: 68th Annual International Meeting, SEG, Expanded Abstracts, 550–553.
———, 1998b, Separation filtering of aeromagnetic data using filterbanks: Exploration Geophysics, **29**, 577–583.
———, 2000, Wavelet compression of an equivalent layer: 70th Annual International Meeting, SEG, Expanded Abstracts, 378–381.
Ridsdill-Smith, T. A., and M. C. Dentith, 1999, The wavelet transform in aeromagnetic processing: Geophysics, **64**, 1003–1013.
Robson, D. F., and R. Spencer, 1997, The New South Wales government's Discovery 2000 — Geophysical surveys and their effect on exploration: Exploration Geophysics, **28**, 296–298.
Roest, W. R., and M. Pilkington, 1993, Identifying remanent magnetization effects in magnetic data: Geophysics, **58**, 653–659.
Roest, W. R., J. Verhoef, and M. Pilkington, 1992, Magnetic interpretation using the 3D analytic signal: Geophysics, **57**, 116–125.
Rosenbaum, J. G., and D. B. Snyder, 1985, Preliminary interpretation of paleomagnetic and magnetic property data from drill holes USW G-1, G-2, GU-3, G-3, and VH-1 and surface localities in the vicinity of Yucca Mountain, Nye County, Nevada: U. S. Geological Survey Open File Report 85-49.
Ross, G. M., J. Broome, and W. Miles., 1994, Potential fields and basement structure: Western Canada Sedimentary Basin, *in* G. D. Mossop and I. Shetsen, comps., Geological atlas of the Western Canada Sedimentary Basin: Canadian Society of Petroleum Geologists and Alberta Research Council, 41–46.
Roux, A. T., 1970, The application of geophysics to gold exploration in South Africa, *in* L. W. Morley, ed., Mining and groundwater geophysics, 1967: Geological Survey of Canada, Economic Geology Report No. 26, 425–438.
Roy, A., 1958, Letter on residual and second derivative of gravity and magnetic maps: Geophysics, **23**, 860–861.
Roy, P. S., J. Whitehouse, P. J. Cowell, and G. Oakes, 2000, Mineral sands occurrences in the Murray Basin, southeastern Australia: Economic Geology, **95**, 1107–1128.
Sabaka, T. J., N. Olsen, and R. A. Langel, 2002, A comprehensive model of the quiet-time, near-the-earth magnetic field: Phase 3: Geophysical Journal International, **151**, 32–68**.**
Sabaka, T. J., N. Olsen, and M. E. Purucker, 2004, Extending comprehensive models of the Earth's magnetic field with Oersted and Champ data: Geophysical Journal International, **159**, 521–547.
Sailhac, P., A. Galdeano, D. Gibert, F. Moreau, and C. Delor, 2000, Identification of sources of potential fields with the continuous wavelet transform: Complex wavelets and application to aeromagnetic profiles in French Guiana: Journal of Geophysical Research, **105**, 19455–19475.
Salem, A., and D. Ravat, 2003, A combined analytic signal and Euler method (AN-EUL) for automatic interpretation of magnetic data: Geophysics, **68**, 1952–1961.
Saltus, R. W., and R. J. Blakely, 1983, HYPERMAG, an interactive, two-dimensional gravity and magnetic modeling program: U. S. Geological Survey Open File Report 83-241.
———, 1993, HYPERMAG, an interactive, 2- and $2\frac{1}{2}$-dimensional gravity and magnetic modeling program, version 3.5: U. S. Geological Survey Open File Report93–287.
Saltus, R. W., P. J. Haeussler, and J. D. Phillips, 2001, Geophysical mapping of subsurface structures in the upper Cook Inlet basin, Alaska: Geological Society of America, Abstracts with Programs, **33**, 345.
Shearer, S., and Y. Li., 2004, 3D inversion of magnetic total gradient data in the presence of remanent magnetization: 74th Annual International Meeting, SEG, Expanded Abstracts, 774–777.
Shi, Z., 1991, An improved Naudy-based technique for estimating depth from magnetic profiles: Exploration Geophysics, **22**, 357–362.

Shuey, R. T., and A. S. Pasquale, 1973, End corrections in magnetic profile interpretation: Geophysics, **38**, 507–512.
Silva, J. B. C., 1986, Reduction to the pole as an inverse problem and its application to low-latitude anomalies: Geophysics, **51**, 369–382.
Silva, J. B. C., and G. W. Hohmann, 1981, Interpretation of three-component borehole magnetometer data: Geophysics, **46**, 1721–1731.
———, 1983, Nonlinear magnetic inversion using a random search method: Geophysics, **48**, 1645–1658.
———, 1984, Airborne magnetic susceptibility mapping: Exploration Geophysics, **15**, 1–13.
Silva, J. B. C., and V. C. F. Barbosa, 2003, Euler deconvolution: Theoretical basis for automatically selecting good solutions: Geophysics, **68**, 1962–1968.
Skeels, D. C., 1967, What is residual gravity?: Geophysics, **32**, 872–876.
Slichter, L. B., 1929, Certain aspects of magnetic surveying: American Institute of Mining and Metallurgical Engineers, Transactions, **81**, 238–260.
Smellie, D. W., 1956, Elementary approximations in aeromagnetic interpretation: Geophysics, **21**, 1021–1040.
Smith, B. D., A. E. McCafferty, and R. R. McDougal, 2000, Utilization of airborne magnetic, electromagnetic, and radiometric data in abandoned mine land investigations, *in* S. E. Church, ed., Preliminary release of scientific reports on the acidic drainage in the Animas River watershed, San Juan County, Colorado: U. S. Geological Survey Open File Report 00-0034, 86–91.
Smith, D. V., and D. Pratt, 2003, Advanced processing and interpretation of the high resolution aeromagnetic survey data over the Central Edwards Aquifer, Texas: Proceedings from the Symposium on the Application of Geophysics to Engineering and Environmental Problems, Environmental and Engineering Society.
Smith, R. A., 1959, Some depth formulae for local magnetic and gravity anomalies: Geophysical Prospecting, **7**, 55–63.
Smith, R. P., V. J. S. Grauch, and D. D. Blackwell, 2002, Preliminary results of a high-resolution aeromagnetic survey to identify buried faults at Dixie Valley, Nevada: Geothermal Resources Council Transactions, **26**, 543–546.
Smith, R. S., J. G. Thurston, T.-F. Dai, and I. N. MacLeod, 1998, ISPI™ — the improved source parameter imaging method: Geophysical Prospecting, **46**, 141–151.
Smock, J. C., 1876, The use of the magnetic needle in searching for magnetic iron ore: Transactions, American Institute of Mining and Metallurgical Engineers (AIME), **4**, 353–362.
Smyth, H. L., 1896, Magnetic observations in geological mapping: American Institute of Mining and Metallurgical Engineers, Transactions, **26**, 640–709.
Spaid-Reitz, M., and P. M. Eick, 1998, HRAM as a tool for petroleum system analysis and trend exploration: A case study of the Mississippi Delta survey, southeast Louisiana: Canadian Journal of Exploration Geophysics, **34**, 83–96.
Spector, A., 1968, Spectral analysis of aeromagnetic data: Ph.D. thesis, University of Toronto.
———, 1971, Aeromagnetic map interpretation with the aid of the digital computer: Canadian Institute of Mining, Metallurgy and Petroleum Bulletin, **64**, 711, 27–33.
Spector, A., and B. K. Bhattacharyya, 1966, Energy density spectrum and autocorrelation function of anomalies due to simple magnetic models: Geophysical Prospecting, **14**, 242–272.
Spector, A., and F. Grant, 1970, Statistical models for interpreting aeromagnetic data: Geophysics, **35**, 293–3302.
———, 1974, Reply to the discussion by G. Gudmunddson on "Statistical models for interpreting aeromagnetic data:" Geophysics, **39**, 112–113.
Spector, A., and W. Parker, 1979, Computer compilation and interpretation of geophysical data, *in* P. J. Hood, ed., Geophysics and geochemistry in the search for metallic ores: Geological Survey of Canada, Economic Report 31, 527–544.
Stavrev, P. Y., 1997, Euler deconvolution using differential similarity transformations of gravity or magnetic anomalies: Geophysical Prospecting, **45**, 207–246.
Stearn, N. H., 1929a, A background for the application of geomagnetics to exploration: Transactions of the American Institute of Mining and Metallurgical Engineers, **81**, 315–345.
———, 1929b, The dip needle as a geological instrument: Transactions of the American Institute of Mining and Metallurgical Engineers, **81**, 345–363.
Steenland, N. C., 1962, Gravity and aeromagnetic exploration in the Paradox basin: Geophysics, **27**, 73–89.
———, 1963a, An evaluation of the Peace River aeromagnetic interpretation: Geophysics, **28**, 745–755.
———, 1963b, Discussion on "An evaluation of basement depth determinations from airborne magnetometer data," by Peter Jacobsen, Jr. (GEO-26-03-0309-0319): Geophysics, **28**, 491–492.
———, 1965, Oil fields and aeromagnetic anomalies: Geophysics, **30**, 706–739.
———, 1998, Reflecting on exploration in the North Sea in the 1960s: The Leading Edge, **17**, 479–482.
Stone, V. C. A., J. D. Fairhead, and W. H. Oterdoom, 2004, Micromagnetic seep detection in the Sudan: The Leading Edge, **23**, 734–737.
Stuart, W. F., 1972, Earth's field magnetometry: Reports of Progress in Physics, **35**, 803–881.
Sweeney, R. E., V. J. S. Grauch, and J. D. Phillips, 2002, Merged digital aeromagnetic data for the Albuquerque and southern Española Basins, New Mexico: U. S. Geological Survey Open File Report 02–205.
Syberg, F. J. R., 1972a, A Fourier method for the regional-residual problem of potential fields: Geophysical Prospecting, **20**, 47–75.
———, 1972b, Potential field continuation between general surfaces: Geophysical Prospecting, **20**, 267–282.
Talwani, M., 1965, Computation with the help of a digital computer of magnetic anomalies caused by bodies of arbitrary shape: Geophysics, **30**, 797–817.
Talwani, M., and J. R. Heirtzler, 1964, Computation of magnetic anomalies caused by two-dimensional structures of arbitrary shape: Stanford University Publications of the Geological Sciences, Computers in the Mineral Industries.
Telford, W. M., L. P. Geldart, and R. E. Sheriff, 1990, Applied geophysics, 2nd ed.: Cambridge University Press.
Teskey, D. J., P. J. Hood, L. W. Morley, R. A. Gibb, P. Sawatzky, M. Bower, and E. E. Ready, 1993, The aeromagnetic survey program of the Geological Survey of Canada; contribution to regional geological mapping and mineral exploration: Canadian Journal of Earth Sciences, **30**, 243–260.
Thompson, D. T., 1982, EULDPH — A new technique for making computer-assisted depth estimates from magnetic data: Geophysics, **47**, 31–37.
Thompson, R., V. J. S. Grauch, D. Sawyer, and M. R. Hudson, 2002, Aeromagnetic expression of volcanic rocks of the Cerros Del Rio volcanic field, Rio Grande rift, north-central New Mexico: Geological Society of America, Abstracts with Programs, **34**, 451–452.
Thurston, J. B., and R. J. Brown, 1994, Automated source-edge location with a new variable-pass horizontal gradient operator: Geophysics, **59**, 546–554.
Thurston, J. B., and R. S. Smith, 1997, Automatic conversion of magnetic data to depth, dip, and susceptibility contrast using the SPI™ method: Geophysics, **62**, 807–813
Thurston, J., J.-C. Guillon, and R. Smith, 1999, Model-independent depth estimation with the SPI™ method: 69th Annual International Meeting, SEG, Expanded Abstracts, 403–406.
Thurston, J. B., R. S. Smith, and J.-C. Guillon, 2002, A multimodel method for depth estimation from magnetic data: Geophysics, **67**, 555–561.
Treitel, S., W. G. Clement, and R. K. Kaul, 1971, The spectral determination of depths to buried magnetic basement rocks: Geophysical Journal of the Royal Astronomical Society, **24**, 415–428.
Tsokas, G. N., and C. B. Papazachos, 1992, Two-dimensional inversion filters in magnetic prospecting: Application to the exploration for buried antiquities: Geophysics, **57**, 1004–1013.
Tsokas, G. N., and R. O. Hansen, 1996, A comparison between inverse filtering and multiple-source Werner deconvolution: 66th Annual International Meeting, SEG, Expanded Abstracts, 1153–1156.
Urquhart, T., 1988, Decorrugation of enhanced magnetic field maps: 58th Annual International Meeting, SEG, Expanded Abstracts, 371–372.
Vacquier, V., N C. Steenland, R. G. Henderson, and I. Zietz, 1951, Interpretation of aeromagnetic maps: Geological Society of America, Memoir 47.
Vallée, M. A., P. Keating, R. S. Smith, and C. St-Hilaire, 2004, Estimating depth and model type using the continuous wavelet transform of magnetic data: Geophysics, **69**, 191–199.
Verduzco, B., J. D. Fairhead, C. M. Green, and C. MacKenzie, 2004, New insights into magnetic derivatives for structural mapping: The Leading Edge, **23**, 116–119.
Vine, F. J., 2001, Reversals of fortune, *in* N. Orestes, ed., Plate tectonics: An insider's history of the modern theory of the Earth: Westview Press, 46–66.
Vine, F. J., and D. H. Matthews, 1963, Magnetic anomalies over oceanic ridges: Nature, **199**, 947–949.
Wang, X., and R. O. Hansen, 1990, Inversion for magnetic anomalies of arbitrary three-dimensional bodies: Geophysics, **55**, 1321–1326.

Wantland, D., 1944, Magnetic interpretation: Geophysics, **9**, 47–58.
Watts, A., 1997, Exploration for nickel in the 90s, or "Til depth us do part:" *in* A. G. Gubins, ed., Proceedings of Fourth Decennial International Conference on Mineral Exploration, Prospectors and Developers Association of Canada, 1003.
Webring, M., 1985, SAKI, A Fortran program for generalized linear inversion of gravity and magnetic profiles: U. S. Geological Survey Open File Report 85-122.
Weinstock, H., and W. C. Overton, eds., 1981, SQUID applications to geophysics: SEG.
Werner, S., 1955, Interpretation of magnetic anomalies of sheet-like bodies, Sveriges Geologiska Undersökning, Series C, Årsbok 43, No. 6.
Whitehill, D. E., 1973, Automated interpretation of magnetic anomalies using the vertical prism model: Geophysics, **38**, 1070–1087.
Whitham, K., and E. R. Niblett, 1961, The diurnal problem in aeromagnetic surveying in Canada: Geophysics, **26**, 211–228.
Wilson, M., and M. Monea, 2004, IEA GHG Weyburn CO_2 Monitoring & Storage Project Summary Report2000–2004: Proceedings of the 7th International Conference on Greenhouse Gas Control Technologies: Petroleum Technology Research Centre.
Wilson, C. R., G. Tsoflias, and M. Bartelmann, 1997, A high-precision aeromagnetic survey near the Glen Hummel Field in Texas; Identification of cultural and sedimentary anomaly sources: The Leading Edge, **16**, 37–44.
Zhang, C., M. F. Mushayandebvu, A. B. Reid, J. D. Fairhead, and M. E. Odegard, 2000, Euler deconvolution of gravity tensor gradient data: Geophysics, **65**, 512–520.
Zietz, I., comp., 1982, Composite magnetic anomaly map of the United States; Part A, Conterminous United States: U. S. Geological Survey Geophysical Investigations Map GP-954-A.
Zietz, I., and G. E. Andreasen, 1967, Remanent magnetization and aeromagnetic interpretation, Mining geophysics, vol. II: Theory: SEG, 569–590.
Zurflueh, E. G., 1967, Applications of two-dimensional linear wavelength filtering: Geophysics, **32**, 1015–1035.